



HAL
open science

Toll-like receptor-2 exacerbates murine acute viral hepatitis

C. Bleau, M. Burnette, Aveline Filliol, Claire Piquet-Pellorce, Michel Samson,
Lucie Lamontagne

► **To cite this version:**

C. Bleau, M. Burnette, Aveline Filliol, Claire Piquet-Pellorce, Michel Samson, et al.. Toll-like receptor-2 exacerbates murine acute viral hepatitis. *Immunology*, 2016, 149 (2), pp.204–224. 10.1111/imm.12627 . hal-01373946

HAL Id: hal-01373946

<https://univ-rennes.hal.science/hal-01373946>

Submitted on 20 Oct 2016

HAL is a multi-disciplinary open access archive for the deposit and dissemination of scientific research documents, whether they are published or not. The documents may come from teaching and research institutions in France or abroad, or from public or private research centers.

L'archive ouverte pluridisciplinaire **HAL**, est destinée au dépôt et à la diffusion de documents scientifiques de niveau recherche, publiés ou non, émanant des établissements d'enseignement et de recherche français ou étrangers, des laboratoires publics ou privés.

Received Date : 18-Feb-2016

Revised Date : 31-May-2016

Accepted Date : 05-Jun-2016

Article type : Original Article

TOLL-LIKE RECEPTOR (TLR)-2 EXACERBATES MURINE ACUTE VIRAL HEPATITIS

Christian Bleau^{*}, Mélanie Burnette^{*}, Aveline Filliol[†], Claire Piquet-Pellorce[†], Michel Samson[†], and
Lucie Lamontagne^{*}

mail id: lamontagne.lucie@uqam.ca

**Department of Biological Sciences, Université du Québec à Montréal, Montreal Canada, H3C 3P8;†*

U.1085 Inserm, IRSET, Institute of Research in Environmental and Occupational Health, Université de

Rennes 1, 35043 Rennes, France

Running title: TLR-2 exacerbates murine acute viral hepatitis

Key words: viral hepatitis- TLR2- inflammation – coronavirus

Abbreviations: Toll-like receptor (TLR), retinoic acid inducible gene (RIG)-1, melanoma differentiation-associated protein (MDA)-5, mouse hepatitis virus (MHV) tumor necrosis factor (TNF)- α , interleukin (IL), transforming growth factor (TGF)- β , interferon (IFN)- α/β , fibrinogen-like protein (Fgl)-2, chemokines CXCL, CCL, natural killer (NK) cells, natural killer (NK)-T cells, Knock-out (KO), alanine aminotransferase (ALT) and aspartate aminotransferase (AST), fluorescence activated cell sorter (FACS), wild type (WT), hepatitis B virus (HBC), hepatitis C virus (HCV), mononuclear cells (MNC), pattern recognition receptor (PRR).

SUMMARY

Viral replication in the liver is generally detected by cellular endosomal TLRs and cytosolic helicase sensors that trigger antiviral inflammatory responses. Recent evidences suggest that surface TLR2 may also contribute to viral detection through recognition of viral coat proteins but its role in the outcome of acute viral infection remains elusive. In this study, we examined *in vivo* the role of TLR2 in acute infections induced by the highly hepatotropic mouse hepatitis virus (MHV) type 3 and weakly hepatotropic MHV-A59 serotype. To address this, C57BL/6 (WT) and TLR2 KO groups of mice were intraperitoneally (i.p) infected with MHV3 or MHV-A59. MHV3 infection provoked a fulminant hepatitis in WT mice, characterized by early mortality and high AST/ALT levels, histopathological lesions and viral replication while infection of TLR2 KO mice was markedly less severe. MHV-A59 provoked a comparable mild and subclinical hepatitis in WT and TLR2 KO mice. MHV3-induced fulminant hepatitis in WT mice correlated with higher hepatic expression of IFN- β , IL-6, TNF- α , CXCL1, CCL2, CXCL10 and alarmin IL-33 than in MHV-A59-infected WT mice and in MHV3-infected TLR2 KO mice. Intrahepatic recruited neutrophils, NK, NK-T cells or macrophages rapidly decreased in MHV3-infected WT mice while they were sustained in MHV-A59-infected WT mice and MHV3-infected TLR2 KO. MHV3 *in vitro* infection of macrophagic cells induced rapid and higher viral replication and/or IL-6 induction in comparison to MHV-A59, depended on viral activation of TLR2 and p38MAPK.. Taken together, these results support a new aggravating inflammatory role for TLR2 in MHV3-induced acute fulminant hepatitis.

INTRODUCTION

Surface or endosomal toll-like receptors (TLR) are key pattern recognition receptors of infectious microorganisms in innate immunity. Host immune recognition of viruses during infections relies mainly on a combination of endosomal Toll-like receptors (TLR-3, 7/8, 9) and cytosolic helicases (RIG-

1 and MDA-5) that sense viral RNA or DNA and trigger signaling pathways leading to inflammatory cytokines, chemokines and antiviral type 1 interferon (IFN α/β) production (reviewed in 1).

Increasing evidences have shown that surface TLRs, such as TLR2 or TLR4, may also trigger acute inflammatory response against viral infections through recognition of viral coat or core proteins (2-5). Activation of surface TLR-dependent signaling pathways leads to the production of various chemokines involved in the recruitment of NK cells, macrophages, neutrophils and B and T cell subsets (reviewed in 5). Higher expression of TLR2 and/or TLR4 and up-regulation of inflammatory factors have been observed in macrophages *in vitro* infected by some viruses such as human immunodeficiency virus (HIV) (6-8), influenza virus (9), hepatitis C virus (HCV) (4), hepatitis B virus (HBV) (10), severe acute respiratory syndrome (SARS) virus (11), and several herpes viruses (12-14). TLR2 and/or TLR4 have also been involved in the induction of high inflammatory responses during acute viral infections. Indeed, TLR2 and TLR4 increase the susceptibility to rotavirus infections in infants (15) and TLR2 was suggested as an aggravating inflammatory factor in herpes virus infections (12, 14).

Recent studies have also reported an overexpression of TLR2 in the liver and on monocytes from HCV- or HCV/HIV-infected patients correlating with hepatic inflammation and damages, suggesting a role for TLR2 in hepatitis-associated inflammation (16, 17). HCV and HBV infections present subclinical to severe acute phase patterns that may lead to viral clearance or evolve towards chronic infections (reviewed in 18). For reasons that are not well understood, few cases of acute infections progress into fulminant hepatic failure, characterized by extensive necrosis and hepatocellular dysfunction, exacerbated inflammation and high mortality rate (19). Hepatic lesions occurring during viral infections are primarily related to viral-triggered host inflammatory response (reviewed in 20) and depend on a poorly elucidated balance between innate immune cells-virus interactions and the control of viral replication that is critical in the outcome of hepatitis. The contribution of TLR2 in

antiviral defenses and inflammatory responses during acute hepatic viral infections is unknown and needs investigation.

The mouse hepatitis viruses (MHV), belonging to coronavirus group, induce acute or subclinical hepatitis, neurological, respiratory or/and enteric diseases in mice according to serotypes (21). The highly hepatotropic MHV3 serotype is a relevant model for studying viral-induced inflammatory disorders during acute hepatic infections as it induces fulminant lethal hepatitis in C57BL/6 mice within 4 days postinfection (p.i.) (22) while the weakly hepatotropic MHV-A59 serotype induces a subclinical hepatitis and is rapidly cleared in the liver (23). Within 72 h of infection, liver dysfunction in MHV3-infected mice results from several foci of extensive necrosis (24) in contrast to that observed in the liver of mice infected with the MHV-A59 serotype (25). All MHV serotypes use the CEACAM1a molecule as viral receptor for infection of host cells through interaction with their viral surface (S) protein (26). It was previously demonstrated that the differential levels of viral replication and hepatitis induced by the MHV serotypes were largely related to the viral S protein (27), suggesting that interactions of the S protein with molecules other than CEACAM1a may reflect their virulence for liver .

Peritoneal macrophages are the first viral cell target during MHV infection, followed by liver cells such as hepatocytes, macrophages, liver sinusoidal endothelial cells (LSECs) and Ito cells (26, 28).

Intrahepatic macrophages, LSECs as well as NK and NK-T cells are considered as major contributors to antiviral responses and cytokines/chemokines release in the liver upon viral infection (29). During MHV3 acute infection, inflammatory mediators such as TNF- α , interleukin (IL)-1, transforming growth factor (TGF)- β , leukotriene B4 and mouse fibrinogen-like (Fgl)-2 protein are strongly produced by infected macrophages, correlating with hepatitis gravity (30). Accordingly, depletion of

macrophages was reported to protect against the fulminance of hepatitis (31), suggesting that exacerbated inflammatory responses are an aggravating factor during MHV3 infection. In addition, the intrahepatic tolerance sustained by IL-4, IL-10, TGF- β and prostaglandin E2 (PGE2) is also disturbed (32). In contrast, it has been suggested that macrophages would rather contribute to the lower gravity of hepatitis and viral clearance during MHV-A59 infection presumably through a rapid type 1 IFN-dependent suppression of viral replication (33). It was demonstrated that the induction of IL-6 and tumor necrosis factor (TNF)- α in peritoneal macrophages infected by MHV3 depended on the fixation of the viral surface (S) protein to TLR2 (34). Previous *in vivo* studies also revealed higher levels of IL-6 and TNF- α in livers from MHV3-infected C57BL/6 mice than TLR2 KO mice, suggesting an inflammatory role for TLR2 in MHV3 infection (34). Thus, the ability of MHVs to ligate and activate TLR2-dependent inflammatory pathways in the liver may represent one determining and differential factor involved in their virulence.

In this study, we demonstrated that the severe acute hepatitis provoked by the highly hepatotropic MHV3 but not by the weakly hepatotropic MHV-A59 serotype, is aggravated by TLR2 in the liver, as demonstrated by significant higher mortality, liver injury, viral replication, levels of inflammatory cytokines and chemokines as well as disturbances in intrahepatic neutrophils, macrophages, NK and NK-T cell recruitment in MHV3-infected WT but not infected TLR2 KO mice or MHV-A59-infected WT mice. Through *in vitro* infection of macrophagic cells, we showed that rapid and higher viral replication and/or IL-6 induction by MHV3, in comparison to MHV-A59 depended on activation of TLR2 and p38MAPK, pointing out macrophages as one source of TLR2-dependent inflammatory responses in MHV3 infection.

MATERIAL AND METHODS

Mice:

Female C57BL/6 (Charles River, St-Constant, Qc, Canada) and TLR2 knock-out (KO)(C57BL/6 background, Jackson Lab., Bar Harbour, MA) mice were housed in a HEPA-filtered air environment. All experiments were conducted with mice between 8 to 10 weeks of age in compliance with the regulations of the Animal Committee of the University of Quebec at Montreal (CIPA-no.641).

Viruses and cells

Highly hepatotropic MHV3 is a cloned substrain isolated from the liver of MHV3-infected DBA2 mice (35). Weakly hepatotropic MHV-A59 serotype was obtained from ATCC (Rockville, MD, USA). Both viruses were produced in L2 cells as previously described (34) and used within 3 passages.

Pathogenic properties of MHV3 were assessed routinely. The mouse fibroblastic L2 cell line used for virus production and titration was grown in RPMI-1640 supplemented with 10% fetal calf serum (FCS) (GIBCO Laboratories, Grand Island, NY) and antibiotics. Murine macrophagic cells J774A.1 (TIB-67™) were grown in RPMI 1640 supplemented with de L-glutamine, antibiotics (GIBCO Laboratories) and 5% FBS (Gemini Bio-Products, Woodland, CA). All cells were passaged before reaching 85% confluence.

In vivo viral infections

Groups of 6-7 wild type C57BL/6 and TLR2 KO mice were infected intraperitoneally (i.p.) with 10^3 TCID₅₀ of MHV3 or MHV-A59. Mock-infected mice received a similar volume of PBS. Clinical signs and survival percentages were recorded and mice were sacrificed when clinical signs reached limit points as determined by CIPA regulations. In other experiments, mice were sacrificed by CO₂ anoxia at 24,

48 and 72h postinfection (p.i.) without regard of clinical signs. Liver and blood samples were collected and processed for further analyses.

Histopathological, transaminase activity and immunohistochemical analyses

The histopathological analysis of liver was done by hematoxylin-eosin-safran staining. Levels of serum ALT and AST transaminases were assessed according to the IFCC primary reference procedures using Olympus AU2700 Autoanalyser[®] (Olympus Optical, Tokyo, Japan).

Immunolocalization of IL-33 or CXCL10 was performed by histochemistry staining using primary goat anti-mouse-IL-33 and anti-CXCL10 (R&D System, Minneapolis, MN) and secondary HRP-conjugated rabbit anti-goat antibody for IL-33 (Dako, Markham, Ont., Canada) and OmniMap anti-Rabbit-HRP (RUO) for CXCL-10 followed by hematoxylin counterstaining in Ventana machine (Ventana Medical Systems, Inc. Tucson, AZ), as previously described (36). Counting of necrosis areas and inflammatory foci was carried out on liver areas 15 to 30 mm² using the NDP.2 view image analysis software (Hamamatsu Photonics K.K., Japan).

In vitro viral infections.

J774A.1 cells were infected with MHV-A59 or MHV3 at a multiplicity of infection (m.o.i.) of 0.1 to 1 or treated with the synthetic bacterial ligand for TLR1/2 (Pam₃CSK4) (InvivoGen, San Diego, CA).

Infections were conducted in a minimal volume of fresh complete medium for the first two hours and then incubated at 37°C in 5% CO₂ atmosphere for various times p.i. according to experiments.

Supernatants were collected and kept at -80°C for subsequent viral titration and/or ELISA tests.

Total cell RNA was extracted from cell culture and prepared for subsequent RT-PCR analysis.

RNA interference treatments.

J774A.1 cells were plated in 24 well plates at 6×10^4 cells per well and transfected with 25nM of mouse CEACAM1 small interfering RNA (siRNA) FlexiTube premix (Qiagen®, Cambridge, MA) (Mm_Ceacam1_3: CAACTCATGCATTCCTACTCTA) and/or mouse TLR2 (Mm_Tlr2_4: CTCGTTCTCCAGCATTTAAA) for at least 24 hours before infection. Negative and positive siRNA controls (AllStars Negative Control siRNA and Ctrl_AllStars_3, respectively, Qiagen), were added to all transfection experiments. Synthetic bacterial ligand for TLR1/2 (Pam₃CSK4) (InvivoGen San Diego, CA) was used as TLR2 positive control for cytokine production.

RNA isolation and RT-qPCR

Total RNA from frozen liver samples of C57BL/6 and TLR2 KO mice was extracted using TRIzol reagent (In Vitrogen, Burlington, Ont., Canada) and residual genomic DNA was removed with the Turbo DNA-free kit (Ambion, Austin, TX). Cell culture RNA was extracted with the NucleoSpin® RNA II kit (Macherey-Nagel GmbH & Co. KG, Düren, Germany). One µg of RNA was retro-transcribed into cDNA using the High capacity cDNA reverse transcription kit (Applied Biosystems, Foster City, CA). Real time PCR amplification was carried out on 25ng cDNA using the HotStart-IT™ SYBR® Green qPCR Master Mix (USB Corporation, Cleveland, OH) on a ABI 7300 system (Applied Biosystems). Threshold cycle values (Ct) were collected and used for “ $\Delta\Delta C_t$ ” analysis. Specific primers for HPRT, MHV-nucleocapsid, TLR-2, TLR-3, -4, -7, MDA-5, RIG-1, IFN- β , IL-6, TNF α , IL-33, Fgl- 2, CXCL1, CXCL10, and CCL2 were used (Table I). The relative gene expression was normalized to HPRT as endogenous control and expressed as a ratio to gene expression in mock-infected mice livers (arbitrarily taken as 1). The specificity of the PCR products was confirmed by melting curve analyses.

ELISA assays

Frozen liver samples from C57BL/6 and TLR2 KO mice were weighted and homogenized in NP40 lysis buffer (In Vitrogen) completed with a protease inhibitor cocktail and 1 mM PMSF (Sigma Aldrich, St-Louis, MA) for protein extraction. Liver suspension was kept on ice for 30 min and centrifuged 10 min at 13000 RPM. Determination of IFN- β (PBL, Piscataway, NJ), IL-6, TNF- α (BD Biosciences, Mississauga, Ont., Canada), and CXCL1, CXCL10, CCL2 (eBiosciences, San Diego, CA) levels in liver lysates or cell culture supernatants was carried out according to the manufacturer's procedure.

p38 MAPK assay.

The p38 MAPK activity has been evaluated in J774A.1 cells plated in 24 well plates at 3×10^4 cells per well 24 h before infections with MHV-A59 or L2-MHV3 at a m.o.i. of 5. At 5, 15, 30, 45 or 60 minutes p.i., supernatants were collected and frozen at -80°C , and the cells were washed three times with cold PBS 1X before RNA and protein extraction. Activity of p38 MAPK in *in vitro* infected cells was evaluated by phosphorylation (T180/Y182) levels with the ELISA ONE™ kit (TGR BioSciences, Thebarton, Australia) according to the manufacturer's indications. Values are expressed as percentage of phosphorylated p38/ total p38 relative to cellular control.

Virus titration

Frozen liver samples from 24 and 72h MHV3- or MHV-A59-infected C57BL/6 or TLR2 KO mice were weighted and homogenized in cold PBS. Suspension was then centrifuged at 13000 RPM for 30 min, 10-fold serial-diluted and tested for viral detection on L2 cells cultured in 96-well plates. Cytopathic effects were recorded at 72h p.i. and virus titers were determined according to Reed-Muench method and expressed as \log_{10} TCID₅₀.

Cytofluorometric studies.

Livers were perfused with PBS through the portal vein to remove blood cell contamination prior to dissection. After homogenization of liver tissue and elimination of hepatocytes by sedimentation, immune cells were purified using 35% Percoll gradient (Sigma Aldrich) and red blood cells were lysed with a Tris-buffered ammonium chloride solution. A million (10^6) of mononuclear cells (MNC) were incubated with anti-CD16/32 antibodies (BD Biosciences) to block non-specific binding. Cells were then incubated with optimal dilutions of anti-CD3-V500, anti-Gr1-V450, anti-CD11b-PE-Cy7, anti-CD19-APC, anti-CD4-FITC, anti-NK1.1-PerCP-Cy-5.5 and anti-CD8-APC-Cy7 antibodies (BD Biosciences) and fixed in PBS containing 2% FCS, 0.01 M sodium azide and 2% formaldehyde. Stained cells were analyzed on a FACS Aria II[®] flow cytometer using BD FACS Diva software (BD Bioscience) and the data were processed using CXP software (Beckman Coulter, Mississauga, Ont, Canada). Dead cells and doublet cells were excluded on the basis of forward and side scatter and analyses were performed on 10,000 events recorded. Myeloid cells, gated by high side scatter, were assessed for CD11b and Gr1 to enumerate macrophages ($CD11b+Gr1^{inter}$) and neutrophils ($CD11b+Gr1^{high}$). Lymphoid cells were gated according to FSC/SCC and first assessed for NK1.1 and CD3 expression to discriminate NK from NKT cells. $CD3+NK1.1-$ T cells were further gated to allow determination of $CD4+$ and $CD8+$ subpopulations. B lymphocytes were determined by $CD19+ CD3-$ expression (Fig. S-1).

Statistical analyses

Data obtained from *in vivo* experiments were expressed as means \pm the standard error of the mean. Multiple group analyses for PCR, ELISA and viral titers data were evaluated by one-way ANOVA test with post-hoc Tukey test using PASW Statistics software (PASW version 18, IBM SPSS Inc. Chicago, IL). Survival curve comparisons were performed using the Log Rank test. Analysis of *in vitro* results

was performed using Student's *t* test to evaluate the statistical significance of differences between infected or treated cells and uninfected or untreated cells. All results are shown as means \pm standard error. Values of $p \leq 0.05$ were considered as significant.

RESULTS

Higher hepatic damages and viral replication in the liver of MHV3- than MHV-A59-infected mice

To confirm that the highly hepatotropic MHV3 induces more dramatic hepatic lesions than the weakly virulent MHV-A59 serotype following i.p. inoculation, groups of C57BL/6 mice were infected with both viruses, livers were collected at 24 to 72 h p.i. and histopathological analysis, viral replication and IFN- β production levels were recorded. Histopathological analysis of livers from MHV3-infected mice revealed few inflammatory cells surrounding necrotic foci as soon as 24h p.i. (Fig.1- sect. I-A). Presence of inflammatory cells, however, was reduced from 48h p.i. while necrotic foci extended until 72h p.i. (Fig.1 sect. I-B and C). No inflammatory foci were observed in livers from mock-infected mice (results not shown). Larger inflammatory foci, however, were observed in liver from MHV-A59-infected mice up to 48h p.i. without extensive necrosis areas as seen in MHV3-infected mice ($p \leq 0.01$) (Fig. 1, sect. I- D to F and G). Extensive hepatic lesions in mice infected by MHV3 correlated with higher levels of AST and ALT transaminases at 72 h p.i. than in MHV-A59 infected mice (Fig. 1- sect. II- A and B) ($p \leq 0.001$).

Viral replication, as evidenced by nucleocapsid RNA levels and viral titers, increased more in the liver of MHV3-infected mice when compared to mice infected with MHV-A59 ($p \leq 0.05$ to 0.001) (Fig. 1 sect. II- C and D). MHV3 replication in the liver increased throughout infection despite higher IFN- β production ($p \leq 0.001$) (Fig. 1 sect. II- E and F). Such lower viral replication of MHV-A59, however, did not result from an increase in IFN- β , since lower mRNA levels and production of IFN- β were detected

in the liver of MHV-A59-infected. No increase in IFN- α transcription has been observed in both MHV3- and MHV-A59- infected mice (results not shown).

Higher expression of TLR2 over other TLRs and helicases in the liver of MHV3- than MHV-A59-infected mice

Several endosomal TLRs and helicases are simultaneously activated and up-regulated upon viral infection, triggering inflammatory responses (reviewed in 1). We explored the hypothesis that MHV3 infection may induce higher expression of TLRs or helicase genes in the liver than MHV-A59. Thus, kinetics of transcription levels of surface TLR-2 and -4, endosomal TLR-3 and -7, and helicase RIG-1 and MDA-5 genes have been assessed by qRT-PCR in the liver of infected mice from 24 to 72 h p.i. and expressed as mRNA fold changes relative to levels in mock-infected mice. As shown in figure 2A, TLR2 gene expression steadily increased over the course of infection with MHV3 reaching over 120-fold the expression in mock-infected mice at 72h p.i. while it remained barely increased and drastically lower in MHV-A59-infected mice ($p \leq 0.05$ to 0.001). Levels of TLR4 and TLR7 mRNA expression were not affected by neither MHV3 nor MHV-A59 infections (Figs 2B and C). Endosomal TLR3 or RIG-1 and MDA-5 gene expression levels also increased in MHV3-infected mice, albeit markedly lesser than TLR2, and were similarly lower or not induced in mice infected with MHV-A59 ($p \leq 0.05$ to 0.001) (Figs 2D, E and F).

These data suggest that MHV3 but not MHV-A59 infection strongly induces expression of TLR2, over other TLRs and helicases, in the liver of infected mice.

Higher expression of inflammatory cytokines, IL-33 (alarmin) and Fgl2 in the liver of MHV3- than MHV-A59 infected mice

Activation of TLRs, mainly surface TLR-2, is involved in the release of proinflammatory cytokines such as TNF- α and IL-6 (reviewed in 1). Higher induction of hepatic TLR2 expression by MHV3 than MHV-A59 infection suggests that higher levels of TNF- α or IL-6 may occur in the liver of MHV3-infected mice. To investigate this hypothesis, levels of TNF- α and IL-6 expression were evaluated by qRT-PCR and ELISA tests in livers from infected mice. As shown in figures 3A and B, IL-6 mRNA and secretion levels increased only in MHV3-infected mice ($p \leq 0.05$ and 0.001). Higher expression of TNF- α was also found in the liver of MHV3- than MHV-A59- infected mice ($p \leq 0.01$ to 0.001) (Fig. 3C) and correlated with higher secretion at 72h p.i. ($p \leq 0.001$) (Fig. 3D).

We have previously demonstrated that expression of IL-33, a new alarmin, was up-regulated in the liver of MHV3-infected C57BL/6 mice correlating with an increase of inflammatory cytokines (36). mRNA levels and immunolocalization for IL-33 were assayed in the liver of MHV3- and/or MHV-A59-infected mice. As shown in figure 3E, gene expression of IL-33 increased only in the liver of MHV3-infected mice ($p \leq 0.001$) and IL-33 was localized mainly in cells lining sinusoids and at a lesser extent in hepatocytes at 24 and 72 h p.i. in MHV3-infected mice (Fig. 3G).

It was previously demonstrated that fulminance of MHV3-induced hepatitis correlated with levels of Fgl-2 produced by liver sinusoidal endothelial cells (37, 38). As expected, Fgl2 expression sooner increased at 48h p.i. in the liver of MHV3- than MHV-A59-infected mice ($p \leq 0.05$ and 0.01).

Activation of TLR2, as other TLRs, is also involved in chemokines production in acute and chronic liver diseases (39, reviewed in 1). We hypothesized that MHV3 infection may favor higher release of chemokines in the liver than MHV-A59 infection. Thus, mRNA and protein levels of CCL2, CXCL1 and CXCL10 were evaluated by qRT-PCR and ELISA tests, respectively, in the liver of infected mice. As shown in figure 4, transcription levels of CCL2 and CXCL10 genes increased over infection time in MHV3-infected mice and reached higher levels at 72 h p.i. than in MHV-A59-infected mice ($p \leq 0.05$ to 0.001) (Figs 4A and C). CCL2 was highly produced in liver from MHV3-infected mice ($p \leq 0.01$ and 0.001) (Fig. 4B). Production of CXCL10 however, was higher in the liver of MHV-A59- than MHV3-infected mice although lower gene expression ($p \leq 0.01$ and 0.001) (Fig. 4D). mRNA and protein levels of CXCL1 higher increased in the liver of MHV3-infected mice than in MHV-A59-infected mice ($p \leq 0.05$ to 0.001) (Figs 4E and F).

Transient and lower recruitment of neutrophils, NK cells and macrophages in the liver of MHV3- than MHV-A59-infected mice

Higher CXCL1, CCL2 and lower CXCL10 levels in the liver of MHV3-infected mice suggest higher recruitment of neutrophils, macrophages, NK and NK-T cells rather than lymphoid cells (reviewed in 40). Smaller or lower inflammatory foci, however, were observed in the liver of MHV3- than MHV-A59-infected mice (see Fig. 1, sect. I B to F) suggesting that inflammatory cell subsets are differentially recruited during MHV3 and MHV-A59 infections. To verify this hypothesis, intrahepatic MNC were isolated from the liver of MHV3- and MHV-A59-infected mice at 24 and 48h p.i., immunolabelled and then phenotyped by cytofluorometric analysis. Percentages and numbers of NK-T (NK1.1+CD3+) and NK (NK1.1+CD3-) cells, neutrophils (CD11b^{hi}Gr1^{hi}), macrophages (CD11b⁺Gr1^{int}) as well as B (CD19+), CD4 (CD3-CD4+) and CD8 (CD3+CD8+) lymphocytes subsets were compared between groups of mice. As shown in figure 5A, percentages of neutrophils (CD11b^{hi}Gr1^{hi}) and macrophages (CD11b⁺Gr1^{int}) rapidly increased at 24h p.i. in MHV3-infected mice in spite of high

individual variation for neutrophils ($p \leq 0.05$ to 0.001). Percentages of NK cells (NK1.1+CD3-) increased only at 48h p.i ($p \leq 0.001$) and NK-T (NK1.1+CD3+) cell percentage decreased at 24h p.i. only ($p \leq 0.001$). Percentages of CD4, CD8 and B lymphocytes decreased in the liver of MHV3-infected mice at 24 and/or 48 h p.i. ($p \leq 0.05$ to 0.001) (Fig. 5B), as previously reported (41).

Analyses of cell subset percentages, however, are not fully representative of recruited inflammatory cells as total number of isolated MNC cells strongly decreased with time in the liver of MHV3-infected mice (41). To properly reflect the evolution of cell recruitment in infected mice, absolute numbers of each inflammatory cell subset have been calculated in using the percentage of each cell subset reported to total number of isolated MNC cells. As shown in figure 5C, the transient increase of neutrophil percentage observed in the liver of MHV3-infected mice was in accordance with the increase in neutrophil numbers at 24 h p.i. only ($p \leq 0.001$). However, low increase of absolute number of macrophages occurred at 48 h p.i. only ($p \leq 0.05$). In addition, both NK-T and NK cell numbers decreased ($p \leq 0.05$ to 0.001) in contrast to that seen in percentages. The decreases in numbers of CD4, CD8 and B cells were magnified when compared with percentages ($p \leq 0.01$ and 0.001) (Figs 5 B and D). The extensive cell necrosis in the liver of MHV3-infected mice at 72 h p.i., however, did not allow us to isolate sufficient number of MNCs for accurate immunolabellings and cytofluorometric analysis.

In livers from MHV-A59-infected mice, however, percentages of neutrophils strongly increased as soon as 24 h p.i. ($p \leq 0.001$) while NK cells transiently increased ($p \leq 0.05$) and NK-T cells decreased ($p \leq 0.01$ and 0.001) (Fig. 5E). Macrophage percentage slightly increased at 48 h p.i. only ($p \leq 0.05$). In contrast to that seen in the liver of MHV3-infected mice, only B cell percentage decreased slightly at 48 h p.i. ($p \leq 0.01$) while CD4 and CD8 lymphocyte percentages remained unchanged (Fig. 5F). The

mononuclear cells number isolated in the liver of MHV-A59-infected mice did not significantly differ from mock-infected mice, in contrast with that seen in MHV3-infected mice. In consequence, variations in absolute numbers of cell subsets did not differ from percentages (results not shown).

Lower liver damages and viral replication in MHV3-infected TLR2 KO mice

We have previously observed that MHV3-induced acute hepatitis was less severe in TLR2 KO mice (34). The comparative study between MHV3 and MHV-A59 infections regarding severity of hepatitis, TLR2 expression level, and inflammatory cytokines and chemokines in liver from infected mice support this hypothesis and suggest that higher virulence of MHV3 may be related with a TLR2-dependent exacerbated inflammatory responses. To verify whether TLR2 is involved in aggravated hepatic damages and viral replication during acute MHV3 infection, groups of wild type (WT) C57BL/6 and TLR2 KO mice were i.p. infected with MHV3 or MHV-A59 and survival rates, liver injury and viral load in the liver were monitored from 24 to 72 h p.i. As shown in figure 6A, mortality rate of MHV3-infected TLR2 KO mice was delayed when compared to infected WT mice as it occurred only from 96 to 120 h p.i. in contrast to WT mice for which mortality reached more than 70% of mice at 72 h p.i. ($p \leq 0.001$). Considering the fulminance of hepatitis, such a statistical significant delay can support a role for TLR2 in pathogenic process of hepatitis. As expected, no mortality was observed in both WT and TLR2 KO mice infected with MHV-A59 (Fig. S-2A). Histopathological analysis of livers from MHV3-infected TLR2 KO revealed inflammatory foci only by 48h p.i. and lesser necrotic foci at 72h p.i. when compared with liver from MHV3- infected WT mice (Fig. 6B compared to Fig 1, sect. I). In livers from MHV-A59-infected TLR2 KO mice, however, few large inflammatory foci, similar to those observed in MHV-A59-infected WT mice were noted (Fig. S-2B). Accordingly, serum AST and ALT transaminase levels were lower in MHV3-infected TLR2 KO than in infected WT mice (Fig. 6 C and D) ($p \leq 0.05$ and 0.001). Hepatic lesions, comparable to that seen in livers from MHV3-infected

WT mice, occurred later in infected TLR2KO mice (results not shown) leading to a delayed mortality of mice.

Viral replication of MHV3 in the liver of infected TLR2 KO, as determined by the expression of the viral nucleoprotein RNA (RT-qPCR) and viral titers, was also lower and delayed when compared to replication in MHV3-infected WT mice (Fig. 6E and F) ($p \leq 0.05$ to 0.001). MHV-A59 replication in liver from TLR2 KO mice, however, was not altered (Fig. S-2C) when compared with infected WT mice.

Dietrich *et al.* (42) have previously reported that TLR2 signaling may lead to IFN- α/β production when TLR2 is internalized in endosome. As shown in figures 6G and H, transcription and production of IFN- β occurred later and reached lower levels in MHV3-infected TLR2 KO mice than in WT mice ($p \leq 0.001$). No significant increase of IFN- α transcription has been observed in both MHV3-infected mouse strains (results not shown).

TLR2 is involved in aggravation of MHV3-induced hepatitis instead of other TLRs or helicase genes

To support the hypothesis that severity of MHV3-induced hepatitis mainly involves TLR2 rather than other PRRs, kinetics of transcription levels of surface TLR2 and 4, endosomal TLR3 and 7, as well as helicase RIG-1 and MDA-5 genes were compared in livers from MHV3-infected WT and TLR2 KO mice. As observed above, an increase of surface TLR2 but not TLR4 gene expression levels over the course of infection by MHV3 was confirmed in the liver of WT mice ($p \leq 0.05$ to 0.001) (Figs 7A and B) while absence of TLR2 induction was validated in infected TLR2 KO mice. Endosomal TLR3 or RIG-1 and MDA-5 but not TLR7 gene expression levels similarly increased in livers from both WT and TLR2

KO mice infected with MHV3 ($p \leq 0.05$ to 0.001) (Figs 7C to F). These data support that MHV3 infection specifically increases expression of TLR2 in the liver of WT mice since other TLRs and helicases are similarly expressed in infected WT and TLR2 KO mice.

Decreases of inflammatory cytokines, alarmin IL-33 but not Fgl2 gene expression in the liver of MHV3-infected TLR2 KO mice

We have previously reported that IL-6 and TNF- α production by peritoneal macrophages *in vitro* infected with MHV3 depends on TLR2 activation by the viral glycoprotein S (34). In order to verify whether TLR2 is specifically involved in the exacerbation of the inflammatory cytokine response during MHV3 infection, as previously observed in Fig. 3, levels of TNF- α and IL-6 expression were compared by qRT-PCR and ELISA tests in MHV3-infected WT and TLR2 KO mice. As shown in figure 8A, mRNA levels of IL-6 increased throughout MHV3 infection in WT mice ($p \leq 0.01$ and 0.001) but were impaired in infected TLR2 KO mice as demonstrated by four-fold lower levels at 72 h p.i. ($p \leq 0.05$). IL-6 secretion increased only in the liver of MHV3-infected WT mice ($p \leq 0.001$) (Fig. 8B). Similarly, lower expression of TNF- α was found in the liver of MHV3-infected TLR2 KO mice than WT mice ($p \leq 0.05$ and 0.001) (Fig. 8C). Such defect in TNF- α mRNA expression correlated with lower production at 72h p.i. ($p \leq 0.001$) (Fig. 8D).

IL-33 gene expression level was delayed to 72 h p.i. in MHV3-infected TLR2 KO mice while it was induced as early as 24 h p.i. in WT mice ($p \leq 0.01$) (Fig. 8E). mRNA levels for Fgl2, however, increased similarly up to 48h p.i. in the liver of both WT and TLR2 KO infected mice ($p \leq 0.05$ and 0.01) (Fig. 8F).

Decreases in CXCL1, CCL2 and CXCL10 levels in the liver of MHV3-infected TLR2 KO mice

It was recently shown that TLR2 signalling network is essential for inflammatory cell recruitment in acute liver injury (39). Accordingly, we hypothesized that TLR2 activation may be involved in the induction of the high chemokine levels observed during MHV3 infection (Fig. 4) but expected it would be decreased in liver from infected TLR2 KO mice. As shown in figures 9A and B, mRNA and protein levels of CXCL1 increased sooner and higher in the liver of MHV3-infected WT mice than TLR2 KO mice ($p \leq 0.05$ to 0.001). Transcription and production levels of CCL2 and CXCL10 also increased over infection time in infected WT mice but were dramatically impaired and delayed in infected TLR2 KO mice ($p \leq 0.05$ to 0.001) (Figs 9C to F). Immunolocalization of CXCL10 showed lower expression in hepatocytes of MHV3-infected TLR2 KO than WT mice at 72 h p.i. (Fig. 9G).

Delayed recruitment of neutrophils, NK cells and macrophages in the liver of MHV3- infected TLR2 KO mice

To verify whether the reduced production of CXCL1, CCL2 and/or CXCL10 in the liver of MHV3-infected TLR2 KO mice involved a lower recruitment of inflammatory cells, intrahepatic MNC cells were isolated from the liver of mock- and MHV3-infected WT and TLR2 KO mice at 24 and 48h p.i., immunolabelled and then phenotyped by cytofluorometric analysis, as indicated above. As shown in figure S-3A, percentages of neutrophils and macrophages increased at 48 h p.i. only in the liver of MHV3-infected TLR2 KO mice ($p \leq 0.001$) while NK and NKT cell percentages remained unchanged. B and CD8 cell percentages, however, decreased in the liver of infected TLR2 KO mice ($p \leq 0.01$ and 0.001) (Fig. S-3B). As no major reduction in total isolated MNCs was observed over time in livers from MHV3-infected TLR2 KO mice in contrast to that seen in MHV3-infected WT mice, changes in percentages for each cell subset reflect similar changes in cell numbers (results not shown).

Taken together, these results suggest that TLR2 favors higher hepatic damages, viral replication and inflammatory response as well as the transient increase in inflammatory cells and losses of NK and NKT cells in the liver only in MHV3-infected WT mice, not in MHV-A59-infected WT mice or MHV3-infected TLR2 KO mice, support an aggravating role for TLR2 in acute hepatitis.

TLR2-dependent viral replication and inflammatory responses in in vitro MHV3-infected macrophages.

We aimed to identify the cells involved in the exacerbated TLR2-dependent inflammatory responses in the liver of MHV3-infected mice. We first investigated whether TLR2 expression was increased in *in vitro* infected macrophages, hepatocytes and LSECs. Preliminary data revealed that both LSECs (manuscript in revision) and macrophages expressed higher TLR2 expression levels upon MHV3 infection. It has been previously demonstrated that macrophages are the first target cell following MHV infection and that lower virulence of MHV-A59 is due to suppression of viral replication by these cells (22, 33). In addition, induction of TNF- α and IL-6 in peritoneal macrophages infected with MHV3 was shown to depend on surface (S) viral protein fixation to TLR2 and heparan sulfate (34) in contrast to MHV-A59 (43). These observations suggest that macrophages may be one cellular source participating in TLR2-dependent inflammatory responses during MHV3 infection.

We first verified whether MHV-A59 and MHV3 differentially replicate and induce cytokine production in macrophages. J774A.1 macrophages were infected with both viruses at 0.1 to 1 m.o.i. for 4 to 24 h p.i. and MHV nucleoprotein (N-MHV) and IL-6 expression were then evaluated. As shown in Fig. 10A, the nucleoprotein RNA expression occurred sooner and reached higher levels in cells infected by MHV3 than MHV-A59 ($p \leq 0.01$ to 0.001). In accordance, viral titers were also higher in MHV3-infected cells (results not shown). Rapid and higher IL-6 transcription levels

occurred in MHV3-infected cells (Fig. 10B) except at 24 h p.i. ($p \leq 0.001$) and correlated with higher production levels (MHV3: 430 ± 45 pg/ml; MHV-A59: 82 ± 15 pg/ml ($p \leq 0.001$)). To verify whether higher replication of MHV3 in macrophages was associated with faster viral entry into cells, immediate-early levels (within 60 min p.i.) of N-MHV RNA levels were evaluated in MHV3 and MHV-A59-infected J774.1 cells. Higher levels of N-MHV mRNA were detected in MHV3-infected cells than in MHV-A59-infected cells, from 5 min p.i. until 60 min p.i. ($p \leq 0.05$ to 0.001) (Fig. 10C).

Since early MAPK p38 activation is involved in early secretion of IL-6 in MHV3-infected peritoneal macrophages (34), the kinetic of p38 MAPK phosphorylation was evaluated within the first 60 min p.i. by ELISA. A TLR2 agonist (Pam3C5K4) was used as positive control for TLR2-dependent induction of p38 MAPK signalling pathway. Results showed in figure 10D indicate that phosphorylated p38 MAPK rapidly increased in cells treated with TLR2 agonist and peaked within 30 min ($p \leq 0.001$). Similar increase, peaking at 30 min, also occurred in MHV3 infected cells ($p \leq 0.05$ to 0.01) while no increase of phosphorylated p38 MAPK was detected in MHV-A59-infected cells. These results suggest that TLR2 may be involved in rapid and higher viral replication and IL-6 secretion in MHV3-infected cells.

To verify this hypothesis, J774.1 cells were next treated with small interfering (si) RNAs for TLR-2 and/or CEACAM1a genes before infection with MHV3 at a m.o.i of 0.1 to 1.0 for 22h. MHV RNA, TLR2 and CEACAM1a fold changes were then evaluated by qRT-PCR and infectious viruses were titrated. Results indicate that MHV-RNA expression decreased in MHV3-infected cells treated with siRNA for CEACAM1a and/or TLR2 ($p \leq 0.01$) (Fig. 10E). Similarly to N-MHV RNA levels, infectious MHV3 virus titers in supernatants of infected J774.1 cells decreased in siCEACAM1a- or siTLR2- or both siCEACAM1a/siTLR-2 treated J774.1 cells when compared with untreated infected cells ($1.2 \times 10^6 \pm$

0.3 x10⁶; 4.5 x10⁵ ± 0.3 x10⁵ and 1.5 x10⁴ ± 0.3 x10⁴ compared with 2.5 x10⁶ ± 0.8 x10⁶ TCID 50/ml, respectively (p ≤ 0.05 to 0.01)). MHV-A59 RNA, however, decreased only in cells treated with siRNA for CEACAM1a (alone or in combination with siRNA for TLR2) (p ≤ 0.01)(Fig. 10E). As expected, TLR2 expression levels increased higher in MHV3-infected macrophages, and such increase was also inhibited following knockdown of one or both CEACAM1a and TLR2 genes (p ≤ 0.001) (Fig. 10F).

To confirm the role of TLR2 in the early induction of IL-6 response by MHV3, IL-6 mRNA fold changes and secretion were assessed in macrophages treated with siRNA for TLR2 and/or CEACAM1a and infected for 5 or 22 h p.i.. As shown in figures 10G and H, knockdown of CEACAM1a and/or TLR2 genes strongly decreased IL-6 transcription and secretion levels by MHV3-infected macrophages, as more evidenced at 5h p.i. (p ≤ 0.001), indicating that IL-6 production depends on both CEACAM1a and TLR2 molecules. The efficiency of siTLR2 treatment and the involvement of TLR2 in IL-6 induction was confirmed by significant decreases of IL-6 expression in cells activated by the TLR2 agonists Pam₃CSK4 (p ≤ 0.01) (Fig. 10G).

DISCUSSION

In this work, we demonstrated for the first time an aggravating role for TLR2 in the acute phase of hepatitis in comparing the fulminant MHV3-induced hepatitis to milder hepatitis induced by the close-related MHV-A59 infection in mice. The involvement for TLR2 in the fulminance of MHV3-induced acute hepatitis was evidenced by earlier mortality and higher hepatic lesions and viral replication in infected WT mice than TLR2 KO mice while subclinical hepatitis induced by MHV-A59 infection was not influenced by TLR2 as mortality rate, hepatic damages and viral titers were comparable in both infected WT and TLR2 KO mice. The severity of hepatitis in MHV3-infected WT mice correlated with higher expression of TLR2, IFN-β, inflammatory cytokines and chemokines and

alarmin IL-33 in the liver. Despite higher chemokine levels, neutrophils, NK, NK-T cells or macrophages were only transiently or weakly recruited in the liver of MHV3-infected WT mice in contrast to delayed but sustained inflammatory cells recruitment in MHV3-infected TLR2 KO or MHV-A59-infected WT mice.

It is the first report showing higher TLR2 expression over other pattern recognition receptors (PRR)s in acute viral hepatitis during the first days of infection. Many PRRs are activated after exposure to hepatotropic viruses, such as endosomal TLR3 or TLR7 and intracytoplasmic helicases RIG-1 or MDA-5, in order to activate IFN type 1 and inflammatory factors. In the livers from MHV3- but not MHV-A59-infected WT mice, we have observed higher expression of TLR2 over other PRRs such as TLR3, RIG-1, MDA-5 or TLR4, suggesting that MHV3 preferentially activates TLR2 transcription. Higher expression of TLR2 has been recently associated with disease progression of hepatitis C (44). Levels of hepatic inflammation in HCV and HCV/HIV infected patients, also correlated with higher transcription of TLR2 and TLR4 genes in the liver (17) suggesting a proinflammatory role for TLR2 in hepatitis. Accordingly, blocking of TLR2 was recently shown to attenuate ConA-induced experimental hepatitis in mice (45). We have observed lower hepatic lesions, viral replication and inflammatory responses in MHV3-infected TLR2 KO mice, indicating that TLR2 may act as an aggravating factor in fulminant hepatitis. However, TLR2KO mice were not protected from MHV3-induced lethal hepatitis, but survival was significantly improved due to delayed occurrence of hepatic necrosis (observations not shown), supporting that other TLR2-independent mechanisms are also involved in the outcome of MHV3 infection. Unlike MHV3, the weakly hepatotropic MHV-A59 showed no ability to increase TLR2 expression in the liver and induced comparable mild hepatitis in WT or TLR2 KO mice, strengthening the importance of TLR2 in MHV3-induced hepatitis.

TLR2 activation, via the MyD88 /NF- κ B-dependent pathway, leads to up-regulation of numerous genes involved in innate host defence such as TNF- α , IL-1 β , IL-6, IFN- γ , chemokines and TLRs expression (reviewed in 46). We have observed that TNF- α and IL-6 increased sooner and higher in the liver of MHV3-infected WT mice than in TLR2KO or MHV-A59-infected mice. It was previously reported that TNF- α activity significantly increases as soon as 24h p.i. during MHV3 infection, even before the virus is detectable in the liver (47), supporting an early activation through an unidentified signaling pathway. Following i.p. infection, MHV3 primarily replicates in peritoneal macrophages and then within liver Kupffer cells and LSECs (48, 49). A role for macrophages in MHV3-induced TLR2-dependent inflammatory responses is supported by *in vitro* infections. Our results indicate that both CEACAM1a and TLR2 are involved in viral replication and early IL-6 expression (as soon as 5h p.i.) in macrophages. Jacques et al. (34) have previously demonstrated that TLR2 and heparan sulfate were involved in the induction of inflammatory cytokines in MHV3-infected macrophages. Our results suggest that higher and earlier TLR2-dependent IL-6 induction by MHV3 may be related to higher and earlier activation of the p38 MAPK pathway by the virus. In addition, since a very early role for the p38 MAPK pathway (within 30 minutes) was reported in viral replication of MHV3 in J774.1 macrophages (50), higher and sooner replication of MHV3 than MHV-A59 may also result from differential activation of this pathway by the viruses. No role for TLR2, however, was reported in viral replication and induction of IL-6 by MHV-A59 (43, 51). Such difference may explain the lower viral load and inflammatory responses in the liver of MHV-A59-infected mice. In addition, preliminary data have shown that UV-inactivated MHV3 viral particles bound more rapidly to macrophage surface (less than 10 min) than UV-inactivated MHV-A59, suggesting that S protein from MHV3 may express higher affinity for TLR2 than MHV-A59.

Hepatocytes and nonparenchymal hepatic cells were also reported to express both the viral receptor CEACAM1a (26) and TLR2 (52, 53). *In vitro* MHV3 infection in hepatocytes leads to rapid cell death (less than 24 h p.i.) and low viral infectious titers and inflammatory cytokine levels which

are barely influenced by siTLR2 treatments (results not shown), suggesting that exacerbated inflammatory response in the liver of MHV3-infected mice does not mostly depend on infected hepatocytes, in spite of extensive necrosis foci. Vascular and tolerant properties of LSECs, however, were disturbed when *in vitro* infected with MHV3 (manuscript in revision). Thus, we can hypothesize that TLR2 fixation of viral infectious particles or free viral S proteins on MHV3 permissive cells, such as Kupffer cells and LSECs, may favor both viral replication and exacerbated inflammatory responses that may contribute to higher liver injury in MHV3-infected mice. Indeed, high levels of TNF- α in the liver are generally associated with extensive necrosis (54), and absence of TNF- α , but not IL-6, was recently shown to significantly reduce hepatic lesions (AST/ALT) and increase the survival of MHV3-infected mice (55).

Following viral replication in macrophages and LSECs, viruses reach hepatocytes leading to rapid extensive syncytia and cell lysis (28). The fulminance of liver lesions indicates that innate antiviral mechanisms cannot control viral infection and inflammatory responses. Type I IFN production by infected cells is the most important antiviral mechanism acting in the first days of infection. Higher IFN- β production, however, was found in the liver of MHV3-infected WT mice than TLR2 KO mice or MHV-A59-infected WT mice. The positive correlation between IFN- β production and viral replication levels may reflect the spreading of viral replication in the liver rather than the efficiency of antiviral effects. Indeed, it was already reported that higher levels of type I IFN were produced simultaneously with higher MHV3 titers by peritoneal macrophages from C57BL/6 mice (56), supporting a negligible role of type I IFN in the control of MHV3 replication. Such explanation is also supported by a positive correlation between low levels of IFN- β and low viral replication in MHV3-infected TLR2 KO mice or MHV-A59-infected WT mice, indicating that lower viral replication does not result from higher production of antiviral IFN- β . In addition, no significant IFN- α expression was induced in the liver of all infected groups of mice (results not shown), indicating no major role for type I IFN in the control of MHV replication and hepatitis. In addition, type I IFN response in mouse

Accepted Article

coronavirus infections depends mainly on TLR3 and helicases RIG-1 or MDA-5 engagement by viral RNAs (57-59). Transcription levels of TLR3, RIG-1 and MDA5 were comparable in livers from both MHV3-infected WT and TLR2 KO mice and lower transcribed in MHV-A59-infected WT mice, suggesting that higher induction of IFN- β by MHV3 infection did not depend on these PRRs. We can thus postulate that higher levels of IFN- β in the liver of MHV3-infected WT mice may result from extensive hepatic infection and/or TLR2 engagement by MHV3. Indeed, Dietrich *et al.* (42) have demonstrated that translocation of TLR2 in endolysosomal compartments following ligand engagement can trigger IFN- β production via the MyD88/IRF-1/IRF-7-dependent pathway in macrophages. Preliminary data revealed increased expression of IRF-7 in livers from MHV3-infected WT mice suggesting activation of this signaling pathway in some hepatic cells. Future work should address this hypothesis. Nevertheless, such interesting potential new role for TLR2 in IFN- β regulation may not be of a major importance in MHV3 infection since no protection against hepatitis seems provided by high IFN- β levels .

TLR2 activation also leads to production of chemokines involved in inflammatory cell recruitment. Sooner and higher production of CXCL1, CCL2, and CXCL10, as seen in the liver of MHV3-infected WT mice, may involve rapid recruitment of neutrophils, macrophages and NK or T cell subsets, respectively (reviewed in 40). As expected, CXCL1 production and concomitant neutrophil recruitment occurred sooner in the liver of MHV3-infected WT mice suggesting that increase in neutrophils may result from early CXCL1 release, as demonstrated by Moles *et al.* (39). The subsequent loss of neutrophils at 48 h p.i., however, did not depend on a decrease of CXCL1 production since levels increased up to 72 h p.i. We can hypothesize that recruited neutrophils may serve as new cell target for viral infection leading to cell apoptosis, such as previously demonstrated for NK cells (60). Work is in progress to clarify the loss of these cells during MHV3 infection. Our data regarding neutrophils slightly differ from those of Xu *et al.* (61) who reported percentage increases

of neutrophils up to 48 h p.i in the liver of MHV3-infected mice. Such apparent discrepancy results from the dramatic decrease in total intrahepatic MNCs, including NK, B and CD4 cells, leading to an apparent increase in neutrophil percentages in spite of a reduction in their absolute number, such as demonstrated in the present work. These authors also linked neutrophil infiltration to a TNF- α -dependent Fgl2 production. Our results do not support this hypothesis since chemokine production and neutrophil infiltration in the liver occurred earlier than Fgl2 induction in MHV3-infected WT mice. Total counts of MNCs in the liver of both MHV3-infected TLR2KO mice and MHV-A59-infected WT mice were not highly altered over infection time and neutrophils numbers steadily increased up to 48 h p.i. supporting a recruitment of these cells despite lower levels of CXCL-1. The delayed and preserved neutrophil pool may thus favor viral clearance and contribute to control acute hepatitis as suggested by lower viral titers, inflammation and damages in these mice. Recent work regarding the respiratory rat coronavirus infection showed that neutrophils were required for an effective antiviral response but could also contribute to lung pathology (62). On the other hand, we cannot exclude that higher levels of chemokines in the liver of MHV3-infected WT mice may also contribute to hepatotoxicity without respect to neutrophil infiltration (63).

We have similarly observed lower macrophage recruitment in the liver of MHV3-infected WT mice than MHV3-infected TLR2 KO and MHV-A59-infected WT mice despite higher production of CCL2. It was previously demonstrated that macrophage expansion in the liver is related to influx of peripheral monocytes facilitated by high levels of CCL2 rather than increase of Kupffer cells (64, reviewed in 65). However, resident and recruited macrophages are permissive to MHV3 infection (48, 49) and we have shown that viral replication in macrophages is increased by TLR2, suggesting that low number of macrophages in the liver of MHV3-infected WT mice result from higher viral replication and subsequent cell lysis. Accordingly, the low presence of inflammatory cells in necrosis foci observed in livers from MHV3-infected WT mice may thus result from virus-induced cell lysis of

recruited MNCs. Lower levels of CXCL-1 and CCL2 in the liver of MHV3-infected TLR2 KO and MHV-A59-infected WT mice involved lower but sustained recruitment of neutrophils and macrophages, suggesting that these cells might be protective rather than deleterious in acute hepatitis process. In agreement, depletion of macrophages in MHV-A59-infected mice has shown to promote lethal fulminant hepatitis within 4 days p.i. (23).

In addition, NK, NK-T, B and T lymphocytes decreased only in the liver of MHV3-infected WT mice despite higher levels of CXCL10. Such reduction may result directly from permissivity of NK and B cells to viral infection, and indirectly from virally-induced lysis of thymic dendritic cells, such as previously reported (60, 66, 67). The larger inflammatory foci observed in the liver of MHV-A59-infected WT mice and MHV3-infected TLR2 KO mice may thus reflect the sustained recruitment of MNCs. On the other hand, high amounts of CXCL10 in the liver has already been associated with apoptosis of human and murine hepatocytes (68), suggesting that high levels of CXCL10 induced by MHV3 may also contribute to hepatic lesions.

Some other inflammatory factors induced by MHV3 infection were less or not dependent on TLR2. Indeed, we have observed that IL-33 release was less influenced by TLR2 and rather reflected the severity of liver damage, such as previously reported (69, 70). We have recently showed that IL-33 expression was up-regulated in the liver of MHV3-infected C57BL/6 mice, mainly in LSECs, vascular endothelial cells and hepatocytes in the first 24 to 32 h p.i. (36). This study also demonstrated that TLR3 was involved in the upregulation of IL-33 in poly (I : C)-treated mice. However, IL-33 expression was higher induced in the liver of MHV3-infected WT mice than in poly (I :C)-treated mice, suggesting that other PRRs might be involved in IL-33 release during MHV3 infection. Our observations suggest that TLR2 might be another candidate involved in early IL-33 induction. The

mechanism(s) by which MHV3 favor(s) IL-33 secretion is pending and need(s) further investigation.

The induction of the vascular factor Fgl2, a prothrombinase promoting microvascular thrombosis and hepatocyte necrosis during MHV3 infection (37, 38) was comparable in WT and TLR2 KO mice and remained low or delayed in MHV-A59 infected WT mice, indicating that this factor is not regulated by TLR2 and not involved in TLR2-exacerbated hepatic damages, in spite of its worsening role in hepatitis outcome.

The present work with animal models of viral hepatitis induced by two close-related serotypes of MHVs highlights the complex interactions between surface TLR2 and intracellular PRRs in the recognition of viral infections and the induction of protective or worsening inflammatory responses during acute infections. The use of the MHV3 model provided new insights into the aggravating role of surface TLR2 in acute viral diseases. Activation of surface TLR signaling pathways has been recently associated with pathogenic process in several viral infections. Indeed, TLR2 and/or 4 are involved in the induction of inflammatory response in SARS, several herpesviruses (HSV-1, varicella, cytomegalovirus), HIV, HBV and HCV, infections (6 to 14). In most cases, TLR2-promoted inflammatory TNF- α , IL-6 or chemokine IL-8 responses are mediated by macrophages (6, 7, 12, 13, 17). The viral mechanisms involved in the activation of TLR2 inflammatory pathways are not clearly elucidated. The ability of MHV3 viral proteins to bind and activate TLR2 signalling is not unique to coronaviruses. Indeed, HBV and HCV core proteins were reported to induce TLR2-dependent activation of NF- κ B, and p38 MAPK and subsequent production of TNF- α , IL-6 and IL-12 in macrophages (71, 72). Thus, one could presume that activation of TLR2 by HCV/HBV core proteins could aggravate hepatic inflammation and damage. In agreement with this hypothesis, an upregulation of TLR2 in the liver and on monocytes, correlating with higher TNF- α levels and necroinflammatory activity in the liver, was reported in patients with hepatitis C (16, 17). Our data demonstrate for the first time that up-regulating the inflammatory activity of TLR2 in the acute

phase of viral hepatitis favors fulminant hepatitis. In humans, fulminant hepatic failure (FHF) is an uncommon clinical condition characterized by extensive hepatic necrosis, severe impairment of liver function and a high mortality rate (19). The most recognized causal agents of FHF are hepatitis viruses (especially HBV) but several non hepatic herpesviruses (herpes simplex virus, cytomegalovirus and varicella) and drugs were also associated with FHF (19). The pathophysiology of FHF is unclear but increasing evidence suggests that regardless the etiological cause of FHF, host's inflammatory response contributes to liver microcirculatory disorders and injury. Accordingly, macrophage activation and inflammatory cytokines were shown to play a key role in FHF (73, 74). Moreover, the core protein from HBV was suggested as a potential initiating factor in patients with fulminant hepatitis B but mechanisms are still elusive (75, 76). Thus, we can propose that strong TLR2-dependent activation of macrophages in the liver by viral proteins from hepatitis or non hepatitis viruses during acute infection may predispose to FHF induction.

Work is in progress to further determine the mechanisms involved in TLR2-dependent increase of inflammatory responses and viral replication in infected intrahepatic resident and recruited cell populations.

Acknowledgments

C. Bleau, M. Burnette, and A. Filliol performed the experiments. C. Piquet-Pellorce has designed cytofluorometric experiments. L. Lamontagne and C. Bleau have designed the study. C. Bleau and L. Lamontagne have written the paper and all authors contributed to revision and corrections of the manuscript. The authors want to acknowledge Pascale Bellaud and Eric Massicotte for their technical assistance within histochemistry and cytofluorometry analyses, and Dr. Anthony Karelis for revising the manuscript.

This work was granted by NSERC from Government of Canada (no.2895-2009). Christian Bleau and Melanie Burnette were supported by NSERC fellowships

Conflict of interest:

The authors indicated no financial or commercial conflict of interest.

REFERENCES

- 1- Broering R, Lu M, Schlaak JF. Role of Toll-like receptors in liver health and disease. *Clin Sci (Lond)*. 2011;121:415-26.
- 2- Villalba M, Hott M, Martin C, Aguila B, Valdivia S, Quezada C, Zambrano A, Concha MI, Otth C. Herpes simplex virus type 1 induces simultaneous activation of Toll-like receptors 2 and 4 and expression of the endogenous ligand serum amyloid A in astrocytes. *Med Microbiol Immunol*. 2012;201:371-9.
- 3- Dolganiuc A, Oak S, Kodys K, Golenbock DT, Finberg RW, Kurt-Jones E, Szabo G. Hepatitis C core and nonstructural 3 proteins trigger toll-like receptor 2-mediated pathways and inflammatory activation. *Gastroenterology*. 2004;127:1513-24.
- 4- Hoffmann M, Zeisel MB, Jilg N, Paranhos-Baccalà G, Stoll-Keller F, Wakita T, Hafkemeyer P, Blum HE, Barth H, Henneke P, Baumert TF. Toll-like receptor 2 senses hepatitis C virus core protein but not infectious viral particles. *J Innate Immun*. 2009;1:446-54.
- 5- Mercin A, Kluwe J, Schwabe RF. Toll-like receptors as target on chronic liver disease. *Gut* 2009;58:704-20.

- 6- Heggelund L, Müller F, Lien E, Yndestad A, Ueland T, Kristiansen KI, Espevik T, Aukrust P, Frøland SS Increased expression of toll-like receptor 2 on monocytes in HIV infection: possible roles in inflammation and viral replication. *Clin Infect Dis.* 2004; 39:264-9.
- 7- Heggelund L, Damås JK, Yndestad A, Holm AM, Müller F, Lien E, Espevik T, Aukrust P, Frøland SS. Stimulation of toll-like receptor 2 in mononuclear cells from HIV-infected patients induces chemokine responses: possible pathogenic consequences. *Clin Exp Immunol.*; 2004; 138:116-21.
- 8- Gekonge B, Giri MS, Kossenkov AV, Nebozyhn M, Yousef M, Mounzer K, Showe L, Montaner LJ. Constitutive gene expression in monocytes from chronic HIV-1 infection overlaps with acute Toll-like receptor induced monocyte activation profiles. *PLoS One.* 2012;7:e41153.
- 9- Karlström A¹, Heston SM, Boyd KL, Tuomanen EI, McCullers JA. Toll-like receptor 2 mediates fatal immunopathology in mice during treatment of secondary pneumococcal pneumonia following influenza. *J Infect Dis.* 2011; 204:1358-6
- 10- Zhao RR, Yang XF, Dong J, Zhao YY, Wei X, Huang CX, Lian JQ, Zhang Y Toll-like receptor 2 promotes T helper 17 cells response in hepatitis B virus infection. *Int J Clin Exp Med.* 2015; ;8:7315-23.
- 11- Dosch SF, Mahajan SD, Collins AR SARS coronavirus spike protein-induced innate immune response occurs via activation of the NF-kappaB pathway in human monocyte macrophages in vitro. *Virus Res.* 2009; 142(1-2):19-27.
- 12- Kurt-Jones EA, Chan M, Zhou S, Wang J, Reed G, Bronson R, Arnold MM, Knipe DM, Finberg RW. Herpes simplex virus 1 interaction with Toll-like receptor 2 contributes to lethal encephalitis. *Proc Natl Acad Sci U S A.* 2004;101:1315-20.

- 13- Wang JP, Kurt-Jones EA, Shin OS, Manchak MD, Levin MJ, Finberg RW. Varicella-zoster virus activates inflammatory cytokines in human monocytes and macrophages via Toll-like receptor 2. *J Virol.* 2005; 79:12658-66.
- 14- .Boehme KW1, Guerrero M, Compton T. Human cytomegalovirus envelope glycoproteins B and H are necessary for TLR2 activation in permissive cells. *J Immunol.* 2006; 177:7094-102
- 15- Xu J, Yang Y, Sun J, Ding Y, Su L, Shao C, Jiang B. Expression of Toll-like receptors and their association with cytokine responses in peripheral blood mononuclear cells of children with acute rotavirus diarrhoea. *Clin Exp Immunol.* 2006; 144:376-81.
- 16- Riordan SM Skinner NA, Kurtovic J, Locarnini S, Mclver CJ, Williams R, Visvanathan K. Toll-like receptor expression in chronic hepatitis C: correlation with pro-inflammatory cytokine levels and liver injury. *Inflamm Res.* 2006;55:279-85.
- 17- Berzsenyi MD, Roberts SK, Preiss S, Woollard DJ, Beard MR, Skinner NA, Bowden DS, Visvanathan K. Hepatic TLR2 & TLR4 expression correlates with hepatic inflammation and TNF- α in HCV & HCV/HIV infection. *J Viral Hepat.* 2011;18:852-60.
- 18- Rehermann B, Nascimbeni M. Immunology of hepatitis B virus and hepatitis C virus infection. *Nat Rev Immunol.* 2005;5:215-29.
- 19- Liu M, Chan WY, McGilvray I, Ning Q, Levy GA. Fulminant viral hepatitis: molecular and cellular basis, and clinical implications. *Exp Rev Mol Med* 2001; 3:1–19.
- 20- Ramadori G, Moriconi F, Malik I, Dudas J. Physiology and pathophysiology of liver inflammation, damage and repair. *J Physiol Pharmacol.* 2008; 59:107-17. 21.
- 21- Weiss SR, Leibowitz JL. Coronavirus pathogenesis. *Adv Virus Res.* 2011;81:85-164.

- 22- Le Prevost C, Levy-Leblond E, Virelizier JL, Dupuy JM. Immunopathology of mouse hepatitis virus type 3 infection. Role of humoral and cell-mediated immunity in resistance mechanisms. *J Immunol.* 1975;114:221-5.
- 23- Wijburg OL, Heemskerk MH, Boog CJ, Van Rooijen N. Role of spleen macrophages in innate and acquired immune responses against mouse hepatitis virus strain A59. *Immunology* 1997;92 :252-8.
- 24- Lamontagne L, Descoteaux JP, Jolicoeur P. Mouse hepatitis virus 3 replication in T and B lymphocytes correlate with viral pathogenicity. *J Immunol.* 1989;142:4458-65.
- 25- Lavi E, Gilden DH, Highkin MK, Weiss SR. The organ tropism of mouse hepatitis virus A59 in mice is dependent on dose and route of inoculation. *Lab Anim Sci.* 1986;36:130-5.
- 26- Godfraind C, Coutelier JP. Morphological analysis of mouse hepatitis virus A-59-induced pathology with regard to viral receptor expression. *Histol Histopathol* 1998;13:181-9.
- 27- Navas S, Seo SH, Chua MM, Das Sarma J, Lavi E, Hingley ST, Weiss SR. Murine coronavirus spike protein determines the ability of the virus to replicate in the liver and cause hepatitis. *J Virol.* 2001;5:2452-7.
- 28- Martin JP, Chen W, Koehren F, Pereira CA. The virulence of mouse hepatitis virus 3, as evidenced by permissivity of cultured hepatic cells toward escape mutants. *Res Virol.* 1994;145:297-302
- 29- Tacke F, Luedde T, Trautwein C. Inflammatory pathways in liver homeostasis and liver injury. *Clin Rev Aller Immunol* 2009;36: 4-12.
- 30- Pope M, Rotstein O, Cole E, Sinclair S, Parr R, Cruz B, Fingerote R, Chung S, Gorczynski R, Fung L, Leibowitz Y, Rao S, Levy G. Pattern of disease after murine hepatitis virus strain 3 infection correlates with macrophage activation and not viral replication. *J Virol.* 1995;69:5252-60.

- 31- Schindler L, Brücher J, Kirchner H. Protection of mice against infection with mouse hepatitis virus type 3 by injection of silica. *Immunobiology*. 1984;166:62-71.
- 32- Jacques A, Bleau C, Martin JP, Lamontagne L. Intrahepatic endothelial and Kupffer cells involved in immunosuppressive cytokines and natural killer (NK)/NK T cell disorders in viral acute hepatitis. *Clin Exp Immunol*. 2008;152:298-310.
- 33- Cervantes-Barragán L, Kalinke U, Züst R, König M, Reizis B, López-Macías C, Thiel V, Ludewig B. Type I IFN-mediated protection of macrophages and dendritic cells secures control of murine coronavirus infection. *J Immunol*. 2009;182:1099-106.
- 34- Jacques A, Bleau C, Turbide C, Beauchemin N, Lamontagne L. Macrophage interleukin-6 and tumour necrosis factor-alpha are induced by coronavirus fixation to Toll-like receptor 2/heparan sulphate receptors but not carcinoembryonic cell adhesion antigen 1a. *Immunology* 2009;128:e181-92.
- 35- Dupuy JM, Rodrigue D. Heterogeneity in evolutive patterns of inbred mice infected with a cloned substrain of mouse hepatitis virus type 3. *Intervirology*. 1981;16:114-7.
- 36- Arshad MI, Patrat-Delon S, Piquet-Pellorce C, L'helgoualc'h A, Rauch M, Genet V, Lucas-Clerc C, Bleau C, Lamontagne L, Samson M. Pathogenic mouse hepatitis virus or poly(I:C) induce IL-33 in hepatocytes in murine models of hepatitis. *PLoS One*. 2013;8:e74278.
- 37- Ding JW, Ning Q, Liu MF, Lai A, Leibowitz J, Peltekian KM, Cole EH, Fung LS, Holloway C, Marsden PA, Yeger H, Phillips MJ, Levy GA. Fulminant hepatic failure in murine hepatitis virus strain 3 infection: tissue-specific expression of a novel fgl2 prothrombinase. *J Virol* 1997;71:9223-30.
- 38- Marsden PA, Ning Q, Fung LS, Luo X, Chen Y, Mendicino M, Ghanekar A, Scott JA, Miller T, Chan CW, Chan MW, He G, Gorczynski RM, Grant DR, Clark DA, Phillips MJ, Levy GA. The

Fgl2/ fibroleukin prothrombinase contributes to immunologically mediated thrombosis in experimental and human viral hepatitis. *J Clin Invest* 2003;112:58–66.

- 39- Moles A, Murphy L, Wilson CL, Chakraborty JB, Fox C, Park EJ, Mann J, Oakley F, Howarth R, Brain J, Masson S, Karin M, Seki E, Mann DA. A tlr2/S100a9/Cxcl-2 signaling network is necessary for neutrophil recruitment in acute and chronic liver injury in the mouse. *J Hepatol*. 2014;60:782-91.
- 40- Oo YH, Shetty S, Adams DH. The role of chemokines in the recruitment of lymphocytes to the liver. *Dig Dis*. 2010;28:31-44.
- 41- Lamontagne L, Lusignan S, Page C. Recovery from mouse hepatitis virus infection depends on recruitment of CD8(+) cells rather than activation of intrahepatic CD4(+)alphabeta(-)TCR(inter) or NK-T cells. *Clin Immunol*. 2001;101:345-56.
- 42- Dietrich N, Lienenklaus S, Weiss S, Gekara NO. Murine Toll-like receptor 2 activation induces type I interferon responses from endolysosomal compartments. *PLoS One*. 2010;5:e10250.
- 43- Zhou H, Zhao J, Perlman S. Autocrine interferon priming in macrophages but not in dendritic cells results in enhanced cytokine and chemokine production after coronavirus infection. *MBio* 2010; 1:e00219-10.
- 44- Tarantino G, Di Cristina A, Pipitone R, Almasio PL, Di Vita G, Craxi A, Grimaudo S. In vivo liver expression of TLR2, TLR3 and TLR7 in chronic hepatitis C. *J Biol Regul Homeost Agents*. 2013;27:233-9.
- 45- Zhou M, Zhu X, Ye S, Zhou B. Blocking TLR2 in vivo attenuates experimental hepatitis induced by concanavalin A in mice. *Int Immunopharmacol*. 2014;21:241-6.
- 46- Melchjorsen J. Learning from the messengers: Innate sensing of viruses and cytokine regulation of immunity—Clues for treatments and vaccines. *Viruses* 2013;5:470-527.

- 47- Devictor D, Décimo D, Sebire G, Tardieu M, Haddchouel M. Enhanced tumor necrosis factor alpha in coronavirus but not in paracetamol-induced acute hepatic necrosis in mice. *Liver* 1992;12:205-8.
- 48- Décimo D, Boespflug O, Meunier-Rotival M, Hadchouel M, Tardieu M. Genetic restriction of murine hepatitis virus type 3 expression in liver and brain: comparative study in BALB/c and C3H mice by immunohistochemistry and hybridization in situ. *Arch Virol*. 1993;130:269-77.
- 49- Pereira CA, Steffan AM, Kirn A. Interaction between mouse hepatitis viruses and primary cultures of Kupffer and endothelial liver cells from resistant and susceptible inbred mouse strains. *J Gen Virol*. 1984;65:1617-20.
- 50- McGilvray ID, Lu Z, Wei AC, Dackiw AP, Marshall JC, Kapus A, Levy G, Rotstein OD. Murine hepatitis virus strain 3 induces the macrophage prothrombinase fgl-2 through p38 mitogen-activated protein kinase activation. *J Biol Chem*. 1998; 273:32222-9
- 51- Mazaleuskaya L, Veltrop R, Ikpeze N, Martin-Garcia J, Navas-Martin S. Protective role of Toll-like Receptor 3-induced type I interferon in murine coronavirus infection of macrophages. *Viruses*. 2012; 4:901-23.
- 52- Schwabe RF, Seki E, Brenner DA. Toll-like receptor signaling in the liver. *Gastroenterology* 2006; 130:1886–1900.
- 53- Matsumura T, Ito A, Takii T, Hayashi H, Onozaki K. Endotoxin and cytokine regulation of toll like receptor (TLR) 2 and TLR4 gene expression in murine liver and hepatocytes. *J Interferon Cytokine Res*. 2000; 20:915–21
- 54- Schümann J, Wolf D, Pahl A, Brune K, Papadopoulos T, van Rooijen N, Tiegs G. Importance of Kupffer cells for T-cell-dependent liver injury in mice. *Am J Pathol*. 2000;157:1671-83.

- 55- Liu J, Tan Y, Zhang J, Zou L, Deng G, Xu X, Wang F, Ma Z, Zhang J, Zhao T, Liu Y, Li Y, Zhu B, Guo B. C5aR, TNF- α , and FGL2 contribute to coagulation and complement activation in virus-induced fulminant hepatitis. *J Hepatol.* 2015;62:354-62.
- 56- Schindler L, Engler H, Kirchner H. Activation of natural killer cells and induction of interferon after injection of mouse hepatitis virus type 3 in mice. *Infect Immun.* 1982;35:869-73.
- 57- Zhao L, Rose KM, Elliott R, Van Rooijen N, Weiss SR. Cell-type-specific type I interferon antagonism influences organ tropism of murine coronavirus. *J Virol* 2011;85:10058-68.
- 58- Roth-Cross JK, Bender SJ, Weiss SR. Murine coronavirus mouse hepatitis virus is recognized by MDA5 and induces type I interferon in brain macrophages/microglia. *J Virol* 2008;82:9829-38.
- 59- Ireland DD, Stohlman SA, Hinton DR, Atkinson R, Bergmann CC. Type I interferons are essential in controlling neurotropic coronavirus infection irrespective of functional CD8 T cells. *J Virol* 2008;82:300-10.
- 60- Lehoux M, Jacques A, Lusignan S, Lamontagne L. Murine viral hepatitis involves NK cell depletion associated with virus-induced apoptosis. *Clin Exp Immunol.* 2004;137:41-51.
- 61- Xu H, Li H, Cao D, Wu Y, Chen Y. Tumor necrosis factor α (TNF- α) receptor-I is required for TNF- α -mediated fulminant virus hepatitis caused by murine hepatitis virus strain-3 infection. *Immunol Lett.* 2014;158:25-32.
- 62- Haick AK, Rzepka JP, Brandon E, Balemba OB, Miura TA. Neutrophils are needed for an effective immune response against pulmonary rat coronavirus infection, but also contribute to pathology. *J Gen Virol.* 2014;95:578-90.
- 63- Stefanovic L, Brenner DA, Stefanovic B. Direct hepatotoxic effect of KC chemokine in the liver without infiltration of neutrophils. *Exp Biol Med* 2005;230:573-86.

- 64- Zimmermann HW, Seidler S, Nattermann J, Gassler N, Hellerbrand C, Zerneck A, Tischendorf JJ, Luedde T, Weiskirchen R, Trautwein C, Tacke F. Functional contribution of elevated circulating and hepatic non-classical CD14CD16 monocytes to inflammation and human liver fibrosis. *PLoS One*. 2010;5(6):e11049.
- 65- Karlmark KR, Wasmuth HE, Trautwein C, Tacke F. Chemokine-directed immune cell infiltration in acute and chronic liver disease. *Expert Rev Gastroenterol Hepatol*. 2008;2:233-42.
- 66- Jolicoeur P, Lamontagne L. Mouse hepatitis virus 3 pathogenicity expressed by a lytic viral infection in bone marrow 14.8+ mu+ B lymphocyte subpopulations. *J Immunol*. 1989;143:3722-30.
- 67- Lamontagne L, Jolicoeur P. Mouse hepatitis virus 3-thymic cell interactions correlating with viral pathogenicity. *J Immunol*. 1991;146:3152-9.
- 68- Sahin H, Borkham-Kamphorst E, Doo NT, Berres ML, Kaldenbach M, Schmitz P, Weiskirchen R, Liedtke C, Streetz KL, Maedler K, Trautwein C, Wasmuth HE. Proapoptotic effects of the chemokine, CXCL 10 are mediated by the noncognate receptor TLR4 in hepatocytes. *Hepatology* 2013;57:797-805.
- 69- Wang J, Zhao P, Guo H, Sun X, Jiang Z, Xu L, Feng J, Niu J, Jiang Y. Serum IL-33 levels are associated with liver damage in patients with chronic hepatitis C. *Mediat Inflamm* 2120;2012:819636.
- 70- Wang J, Cai Y, Ji H, Feng J, Ayana DA, Niu J, Jiang Y. Serum IL-33 Levels Are Associated with Liver Damage in Patients with Chronic Hepatitis B. *J Interferon Cytokine Res* 2012;32:248-53.
- 71- Cooper A, Tal G, Lider O, Shaul Y. Cytokine induction by the hepatitis B virus capsid in macrophages is facilitated by membrane heparan sulfate and involves TLR2. *J Immunol*. 2005;175:3165-76.

- 72- Dolganiuc A, Oak S, Kodys K, Golenbock DT, Finberg RW, Kurt-Jones E, Szabo G. Hepatitis C core and nonstructural 3 proteins trigger toll-like receptor 2-mediated pathways and inflammatory activation. *Gastroenterology* 2004; 127:1513–24.
- 73- Ando K, Moriyama T, Guidotti LG, Wirth S, Schreiber RD, Schlicht HJ, Huang SN, Chisari FV. Mechanisms of class I restricted immunopathology. A transgenic mouse model of fulminant hepatitis. *J Exp Med* 1993; 178:1541-1554.
- 74- de la Mata M, Meager A, Rolando N, Daniels HM, Nouri-Aria KT, Goka AK, Eddleston AL, Alexander GJ, Williams R. Tumour necrosis factor production in fulminant hepatic failure: relation to aetiology and superimposed microbial infection. *Clin Exp Immunol* 1990; 82:479-48
- 75- Mondelli M, Eddleston AL. Mechanisms of liver cell injury in acute and chronic hepatitis B. *Semin Liver Dis* 1984; 4:47-58.
- 76- Aritomi T, Yatsushashi H, Fujino T, Yamasaki K, Inoue O, Koga M, Kato Y, Yano M. Association of mutations in the core promoter and precore region of hepatitis virus with fulminant and severe acute hepatitis in Japan. *J Gastroenterol Hepatol.* 1998; 13:1125-32.

LEGENDS OF FIGURES

Figure 1: Mortality, hepatic damages and viral replication during MHV3- and MHV-A59-induced hepatitis in C57BL/6 mice. Groups of 6 or 7 C57BL/6 mice were intraperitoneally (i.p.) infected with 1000 TCID₅₀ (tissue culture infective dose 50%) of MHV3 or MHV-A59. Percentages of surviving mice were recorded at various times post-infection (p.i.). Section I-A to F: Histopathological analysis was conducted on livers at 24, 48 and 72 h p.i. Section I-G: Histological analysis of inflammatory foci in liver from MHV3- or MHV-A59 infected C57BL/6 mice. Section II: Serum samples from infected mice were assayed for AST and ALT activity from 24 to 72 h p.i. (A and B). MHV3 or MHV-A59 replication

in livers of infected mice was determined by analysis of the nucleoprotein (MHV-N) RNA expression from 24 to 72 h p.i. by RT-qPCR, and values represent fold change in gene expression relative to mock-infected mice after normalisation with HPRT expression (C). Viral titration (TCID₅₀) in liver was assayed at 24 and 72 h p.i. (D). mRNA fold increases for IFN-β were evaluated by qRT-PCR in livers of MHV3- or MHV-A59 infected mice. Values represent fold change in gene expression relative to mock-infected mice (arbitrary value of 1) after normalisation with HPRT expression (E). Production levels of IFN-β were quantified by ELISA test at 72 h p.i. in livers (F). Results are representative of two different experiments (**P* < 0.05; ***P* < 0.01; ****P* < 0.001)

Figure 2: mRNA levels of TLR-2, TLR-4, TLR-3, TLR-7 and helicases MDA-5 and RIG-1 genes in the liver of MHV3- and MHV-A59-infected mice. Groups of 6 or 7 C57BL/6 (WT) mice were i.p. infected with 1000 TCID₅₀ of MHV3 or MHV-A59. At 24, 48 or 72 h p.i., livers from each group were collected and Toll-like receptors (TLR-2,-3,-4,-7) (A to D) and helicases (MDA5 and RIG-1) (E and F) mRNA fold changes were analyzed by qRT-PCR. Values represent fold change in gene expression relative to mock-infected mice (arbitrary value of 1) after normalisation with HPRT expression. Results are representative of two different experiments. (**P* < 0.05; ***P* < 0.01; ****P* < 0.001).

Figure 3: mRNA levels and production of inflammatory cytokines, IL-33 and fibrinogen-like 2 (Fgl2) in the liver of MHV3- and MHV-A59-infected mice. Groups of 6 or 7 C57BL/6 mice were i.p. infected with 1000 TCID₅₀ of MHV3 or MHV-A59. At 24, 48 or 72 h p.i., livers from each group were collected and mRNA fold increases for IL-6 (A), TNF-α (C) and IL-33 (E) or Fgl2 (F) were evaluated by qRT-PCR in livers of infected mice. Values represent fold change in gene expression relative to mock-infected mice (arbitrary value of 1) after normalisation with HPRT expression. Production levels of IL-6 (B) and TNF-α (D) were quantified by ELISA test at 72 h p.i. in livers. Expression of IL-33 determined by

immunohistochemistry in livers from mock-infected and MHV3-infected WT mice at 24 and 72 h p.i.

(G). Some positive IL-33 cells are indicated by arrows. Results are representative of two different experiments. (* $P < 0.05$; ** $P < 0.01$; *** $P < 0.001$)

Figure 4: mRNA expression and production of chemokines CCL2, CXCL1 and CXCL10 in the liver of MHV3- and MHV-A59-infected mice. Groups of 6 or 7 C57BL/6 mice were i.p. infected with 1000 TCID₅₀ of MHV3 or MHV-A59. At 24, 48 or 72 h p.i., livers from each group were collected. mRNA expression levels for CCL2 (A), CXCL10 (C) and CXCL1 (E) were evaluated by qRT-PCR at 24, 48 and 72 h p.i in livers from MHV3- or MHV-A59-infected mice. Values represent fold change in gene expression relative to mock-infected mice (arbitrary value of 1) after normalisation with HPRT expression. Protein levels of CCL2 (B), CXCL10 (D) and CXCL1 (F) were quantified in livers by ELISA test at 72 h p.i. (* $P < 0.05$; ** $P < 0.01$; *** $P < 0.001$).

Figure 5: Analysis of intrahepatic MNC cells in the liver of MHV3- and MHV-A59-infected C57BL/6 mice. Intrahepatic MNC cells were isolated from groups of 6 mock-infected, MHV3- and MHV-A59-infected C57BL/6 mice at 24 and 48 h p.i., immunolabelled with NK1.1, CD3, Gr1, CD11b, CD19, CD4 and CD8 monoclonal antibodies and analyzed by cytofluorometry. Percentages of NK-T (NK1.1+CD3+), NK (NK1.1+CD3), neutrophils (Gr1^{hi} CD11b^{hi}) and macrophages (Gr1⁺ CD11b^{int}) cells were evaluated in the liver of MHV3- (A) and MHV-A59 (E)-infected mice. Percentages of B (CD19+), and CD4 (CD3+CD4+) and CD8 (CD3+CD8+) subpopulations of CD3+ NK1.1- cells were similarly analyzed (B and F). Absolute numbers for each cell subset were calculated in using respective percentages reported to total number of isolated MNC in the liver of MHV3- (C and D) .(* $P < 0.05$; ** $P < 0.01$; *** $P < 0.001$).

Figure 6: Hepatic damages, viral replication and IFN- β production in the liver of MHV3-infected

WT and TLR2KO mice. Groups of 6 to 7 C57BL/6 (WT) and TLR2 KO mice were i.p. infected with 1000

TCID₅₀ of MHV3. Survival curve of MHV3-infected WT and TLR2KO mice (A). Histopathological analysis was conducted on livers from MHV3-infected TLR2KO at 24, 48 and 72 h p.i. (B). Serum samples from MHV3-infected WT and TLR2 KO mice were assayed for AST (C) and ALT (D) activity at 24 to 72 h p.i. Replication of MHV3 in livers of infected mice was determined by analysis of the nucleoprotein (MHV-N) RNA expression at 24, 48 and 72 h p.i. by RT-qPCR, and by viral titration (TCID₅₀) at 24 and 72 h p.i. (E and F). mRNA fold increases for IFN- β were analyzed in livers from MHV3-infected mice by qRT-PCR at 24, 48 and 72 h p.i. (G). Values represent fold change in gene expression relative to mock-infected mice (arbitrary value of 1) after normalisation with HPRT expression. Protein levels of IFN- β in the liver were quantified by ELISA test at 72 h p.i. (H). (* P < 0.05; ** P < 0.01; *** P < 0.001).

Figure 7: mRNA levels of TLRs and helicases in the liver of MHV3-infected WT and TLR2 KO mice.

Groups of 6 or 7 C57BL/6 (WT) and TLR2 KO mice were i.p. infected with 1000 TCID₅₀ of MHV3. At 24, 48 or 72 h p.i., livers from each group were collected and Toll-like receptors (TLR-2, -3, -4, -7) (A to D) and helicases (MDA5 and RIG-1) (E and F) mRNA fold changes were analyzed by qRT-PCR. Values represent fold change in gene expression relative to mock-infected mice (arbitrary value of 1) after normalisation with HPRT expression. (* P < 0.05; ** P < 0.01; *** P < 0.001). N.D. not done

Figure 8: Expression levels of cytokines, IL-33 and fibrinogen-like 2 (Fgl2) gene in the liver of

MHV3-infected WT and TLR2 KO mice. Groups of 6 or 7 C57BL/6 (WT) and TLR2 KO mice were i.p. infected with 1000 TCID₅₀ of MHV3. At 24, 48 or 72 h p.i., livers from each group were collected. mRNA fold increases for IL-6 (A), TNF- α (C), IL-33 (E), and the Fgl2 (F) were evaluated by qRT-PCR in

livers of infected mice. Values represent fold change in gene expression relative to mock-infected mice (arbitrary value of 1) after normalisation with HPRT expression. Production levels of IL-6 (B) and TNF- α (D) were quantified in livers by ELISA test at 72 h p.i.. (* P < 0.05; ** P < 0.01; *** P < 0.001).

Figure 9: mRNA expression levels and production of CCL2, CXCL1 and CXCL10 in the liver of MHV3-infected WT and TLR2 KO mice. Groups of 6 or 7 C57BL/6 (WT) and TLR2 KO mice were i.p. infected with 1000 TCID₅₀ of MHV3. At 24, 48 or 72 h p.i., livers from each group were collected. mRNA expression for CXCL1 (A), CCL2 (C) and CXCL10 (E) genes was evaluated by qRT-PCR in livers from MHV3-infected WT and TLR2 KO mice. Values represent fold change in gene expression relative to mock-infected mice (arbitrary value of 1) after normalisation with HPRT expression. Protein levels of CXCL1 (B), CCL2 (D) and CXCL10 (F) in the liver were quantified by ELISA test at 72 h p.i. Immunolocalization of CXCL10 in the liver determined by histochemistry staining in MHV3-infected WT and TLR2 KO mice (G). (* P < 0.05; ** P < 0.01; *** P < 0.001).

Figure 10: *In vitro* MHV3 and MHV-A59 infections of macrophages untreated or treated with siRNA for TLR2 and CEACAM1a. J774A.1 macrophages were infected with 0.01 to 1 m.o.i. of MHV3 or MHV-A59 and incubated for various times p.i. according to experiments (A to D). Cells were also transfected with mouse CEACAM1 and/or TLR2 small interfering RNA (siRNA) for at least 24 hours before infections in other experiments (E to F). Nucleocapsid RNA (A, C and E), TLR2 (F), and IL-6 (B and G) mRNA fold changes were analyzed by qRT-PCR at various times p.i. Values represent fold change in gene expression relative to mock-infected mice (arbitrary value of 1) after normalisation with HPRT expression. Phosphorylated p38MAPK levels were evaluated by ELISA test and expressed as percentages of total p38MAPK (D). The synthetic bacterial ligand for TLR2-TLR1 (Pam₃CSK4) was

used as TLR2 positive control for the detection of phosphorylated p38MAPK and IL-6 expression (D and G). IL-6 secretion was quantified by ELISA test in MHV3-infected cells at 5h p.i. (H). Results are representative of two different experiments. (* $P < 0.05$; ** $P < 0.01$; *** $P < 0.001$). N.D. Not done.

TABLE I : Primer sets used for quantitative reverse transcription-PCR

| Gene | Forward primer | Reverse primer |
|---------------|---------------------------------|--------------------------------|
| HPRT | 5'-GAAAGACTTGCTCGAGATGTCATG-3' | 5'-CACACAGAGGGCCACAATGT-3' |
| IFN- β | 5'-CGGACTTCAAGATCCCTATGGA-3' | 5'-TGGCAAAGGCAGTGTAACCTCTC-3' |
| IL-6 | 5'-TCGGAGGCTTAATTACACATGTTCT-3' | 5'-TGCCATTGCACAACCTTTTTCT-3' |
| TNF- α | 5'-TCCCAGGTCTCTTCAAGGGA-3' | 5'-GGTGAGGAGCACGTAGTCGG-3' |
| CCL2 | 5'-GCAGCAGGTGTCCCAAAGAA-3' | 5'-GGTCAGCACAGACCTCTCTCTTG-3' |
| CXCL10 | 5'-GGCCATAGGGAAGCTTAAAAT-3' | 5'-TCGTGGCAATGATCTCAACAC-3' |
| TLR2 | 5'-CCCTGTGCCACCATTTC-3' | 5'-CCACGCCACATCATTCTC-3' |
| TLR3 | 5'-TGGGCTGAAGTGGACAAATCT-3' | 5'-TGCCGACATCATGGAGGTT-3' |
| TLR4 | AGCTTCAATGGTGCCATCATT | CCAGGTGCTGCAGCTCTTCT |
| TLR7 | 5'-CAGTGAACCTGGCCGTTGA-3' | 5'-CAAGCCGTTGTTGGAGAA-3' |
| MHV-N | 5'-TGGAAGGTCTGCACCTGCTA-3' | 5'-TTTGCCACCGGATTG-3' |
| RIG-I | 5'-GCCAGAGTGTCAGAATCTCAGTCAG-3' | 5'-GAGAACACAGTTGCCTGCTGCTCA-3' |
| MDA-5 | 5'-GCCCTCCTCCTCTGAGACT-3' | 5'-GCTGGAGGAGGGTCAGCAA-3' |
| IL-33 | 5'-GCTGCGTCTGTTGACACATTG-3' | 5'-GGGAGGCAGGAGACTGTGTAA-3' |
| Fgl2 | 5'-CGTTGTGGTCAACAGTTTGA-3' | 5'-GATGTTGAACCGGCTGTGACT-3' |
| CXCL1 | 5'-CCGAAGTCATAGCCACACTCAA-3' | 5'-CAAGGGAGCTTCAGGGTCAA-3' |

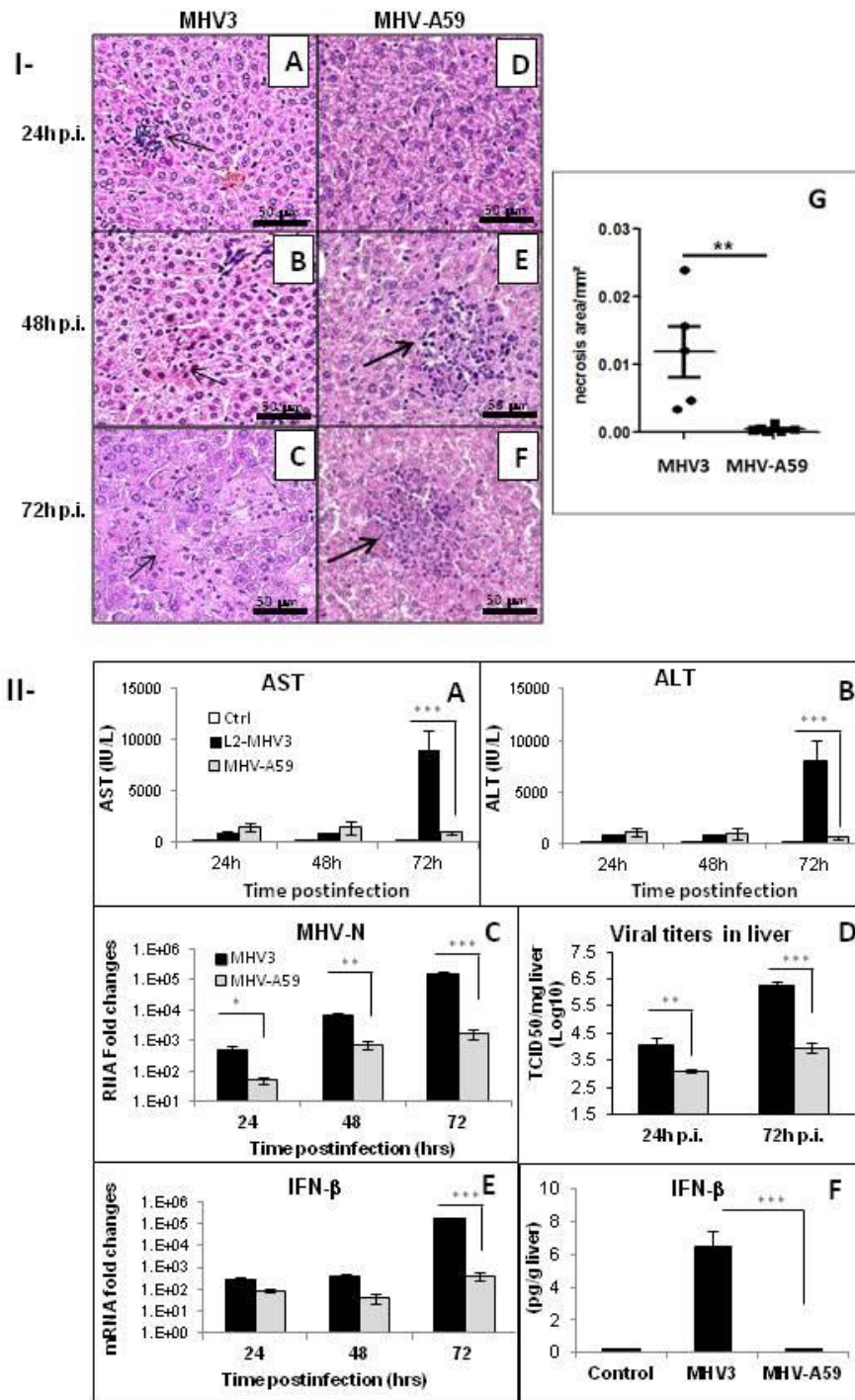


Figure 1

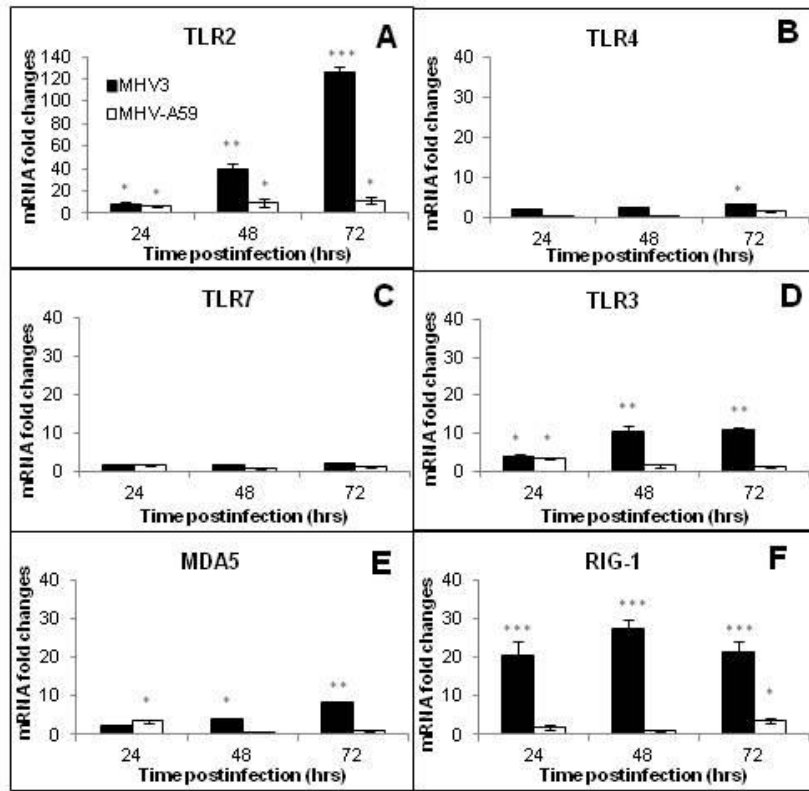


Figure 2

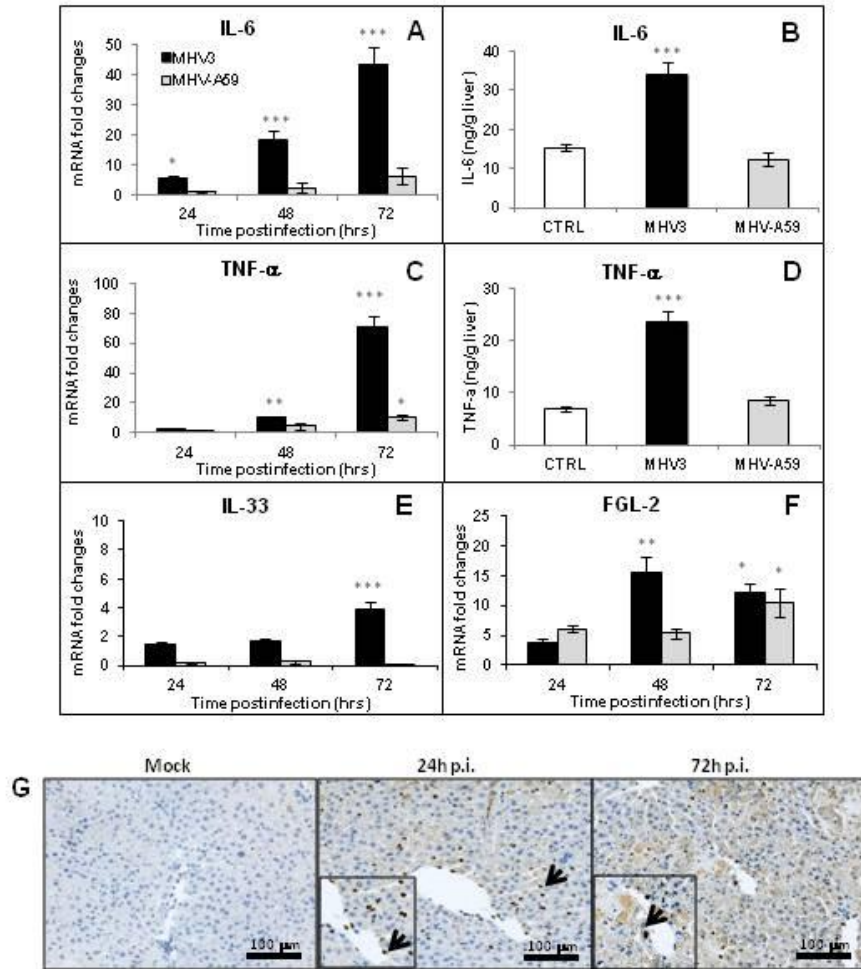


Figure 3

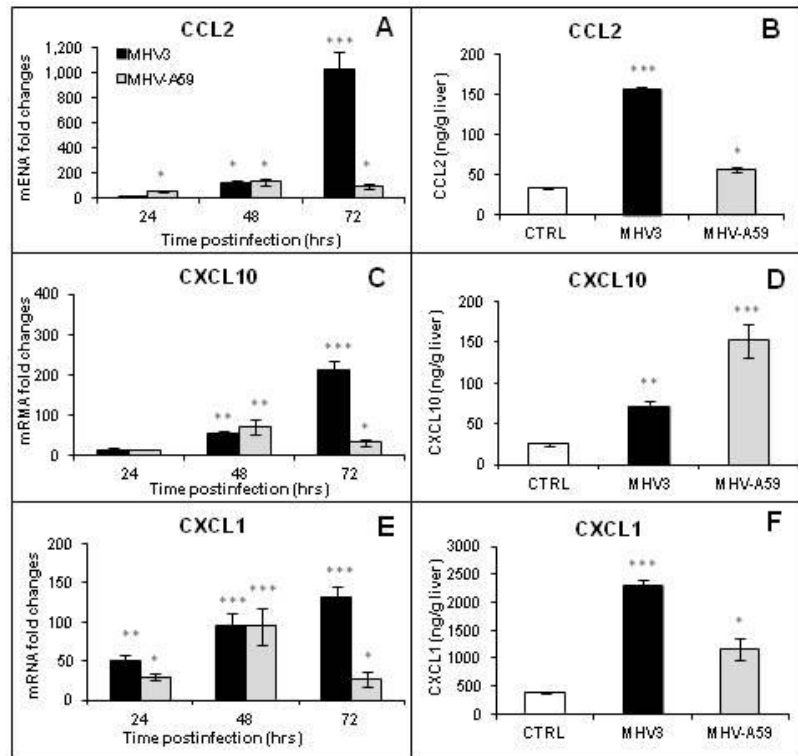


Figure 4

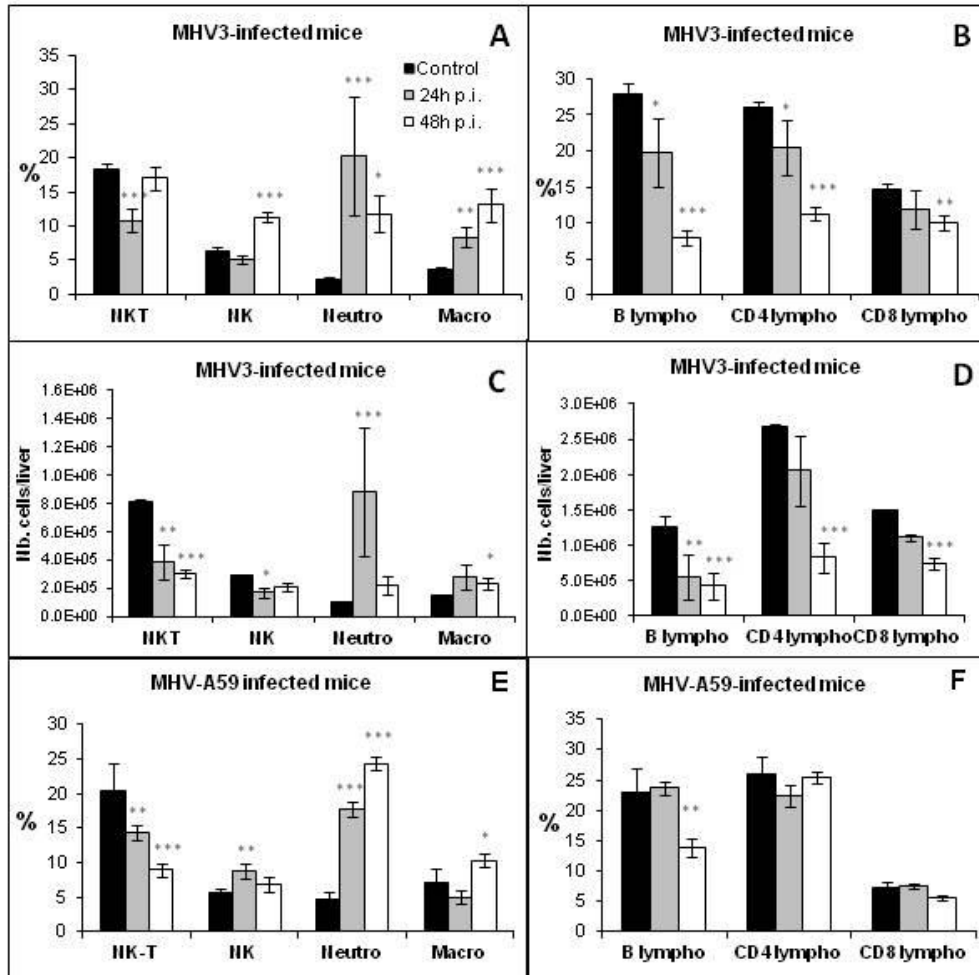


Figure 5

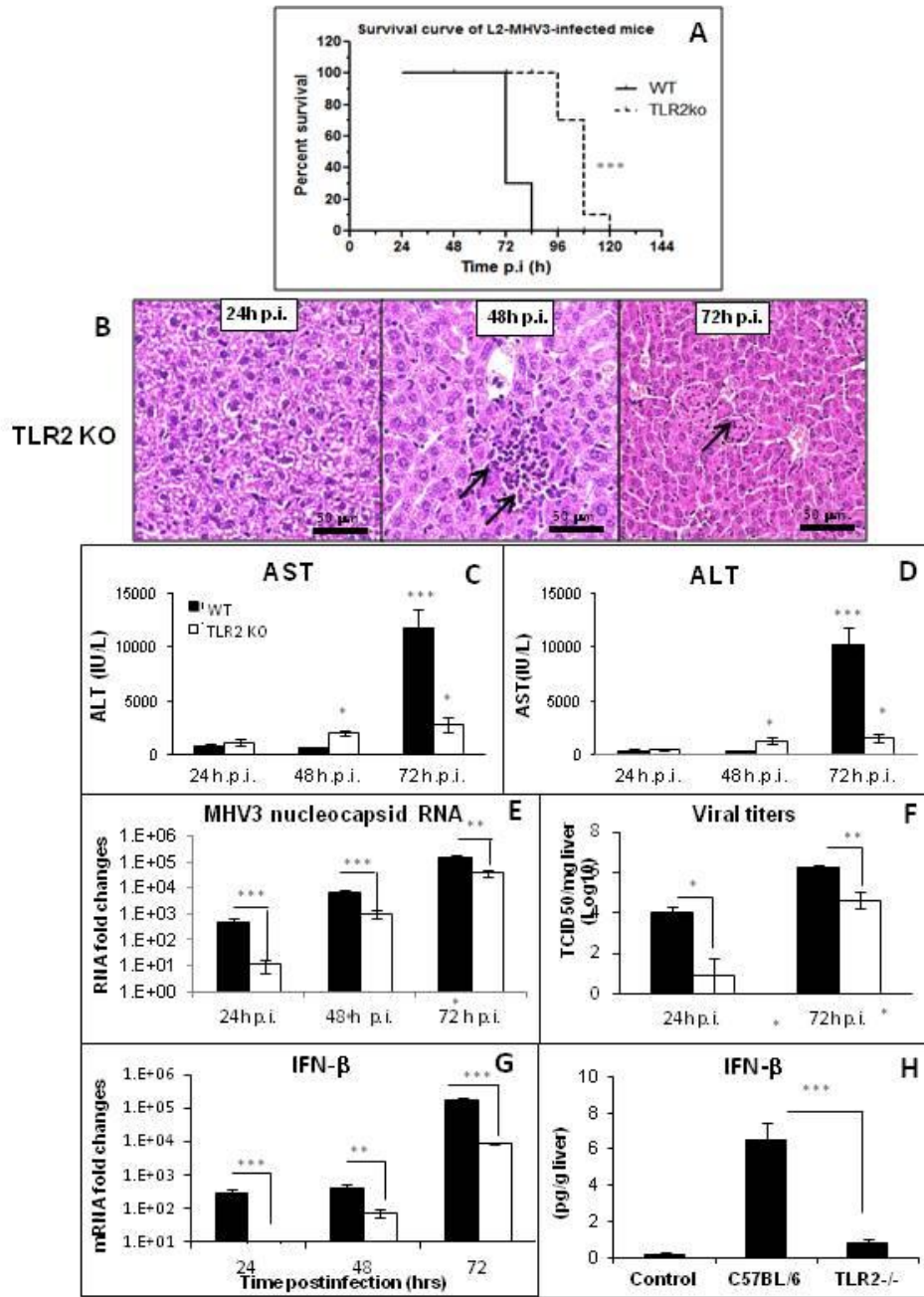


Figure 6

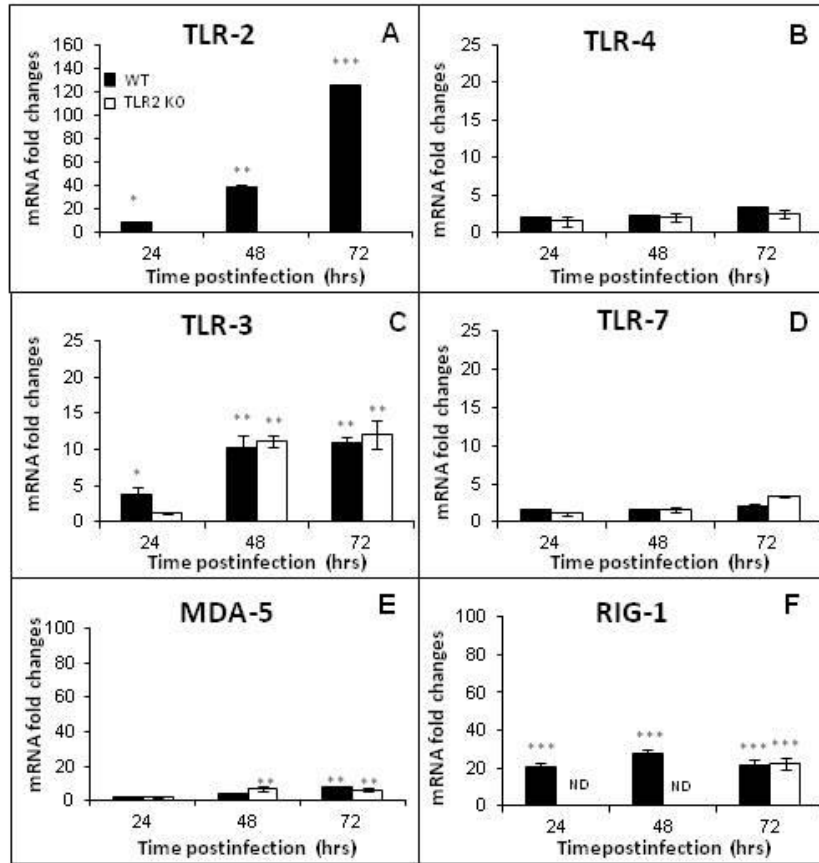


Figure 7

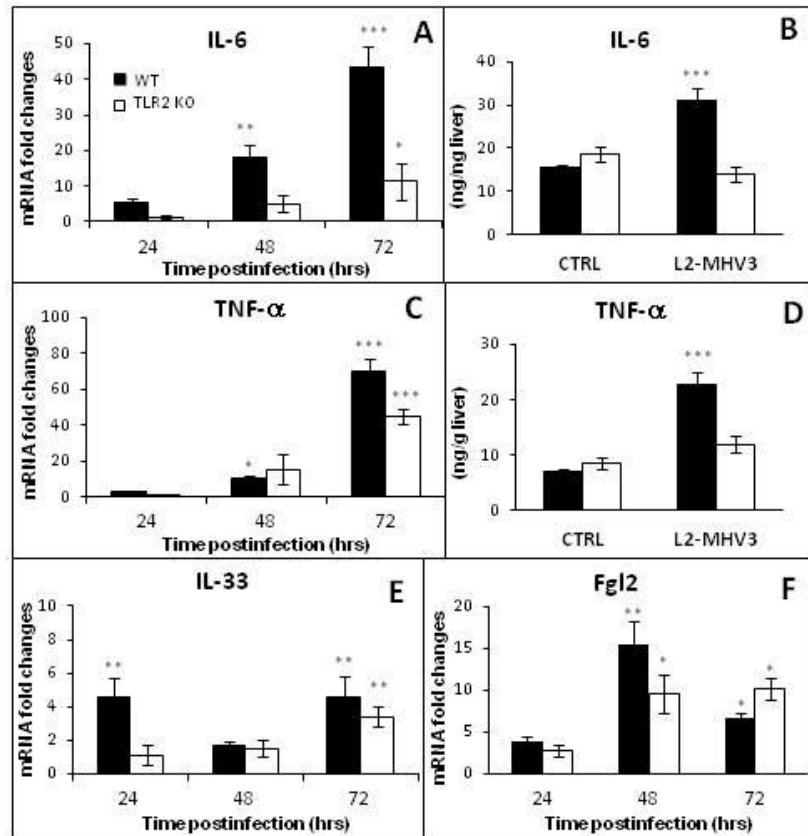


Figure 8

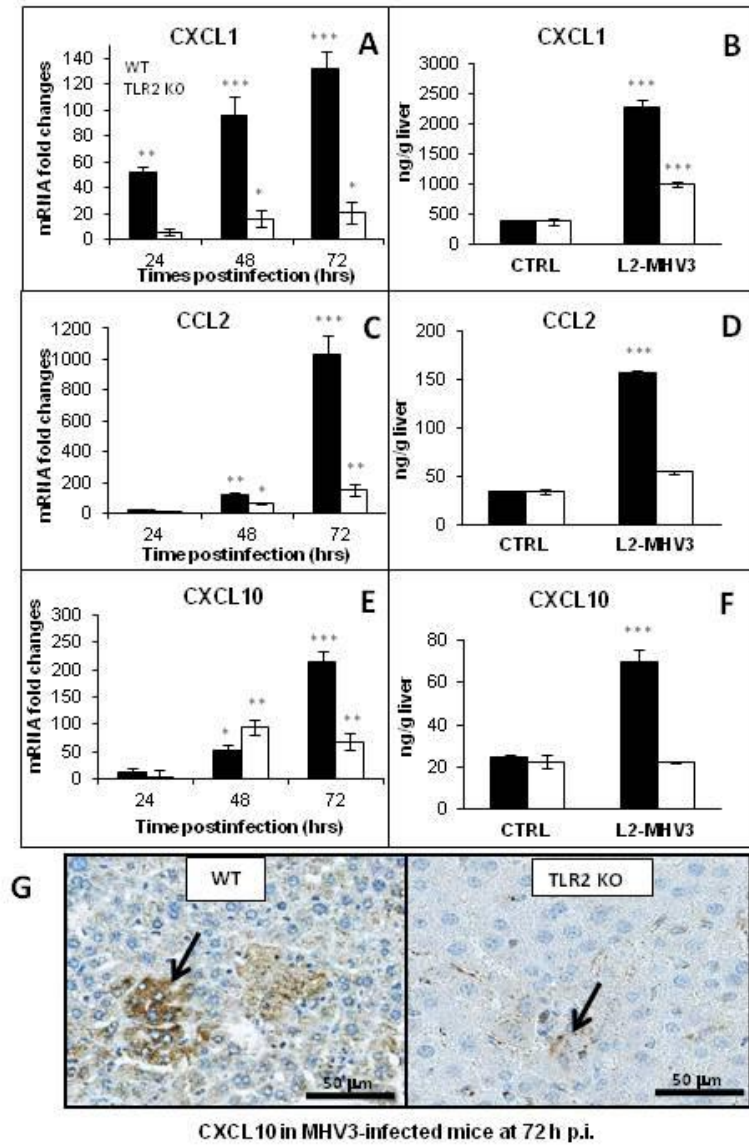


Figure 9

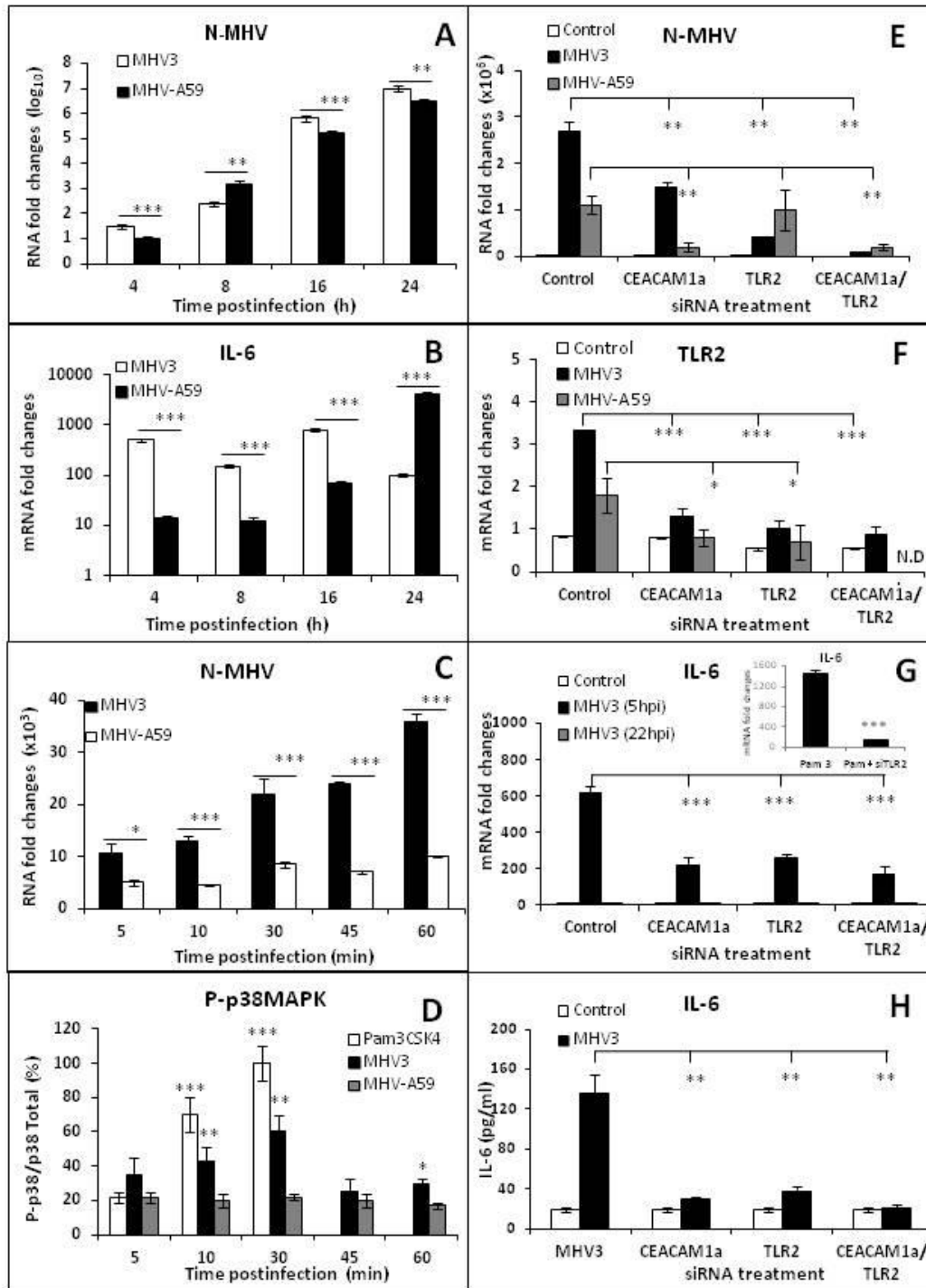


Figure 10